

Biwhitening Reveals the Rank of a Count Matrix

Boris Landa^{1,*} Thomas T.C.K. Zhang² Yuval Kluger^{1,3,4}

¹Program in Applied Mathematics, Yale University

²Department of Electrical and Systems Engineering, University of Pennsylvania

³Interdepartmental Program in Computational Biology and Bioinformatics, Yale University

⁴Department of Pathology, Yale University School of Medicine

*Corresponding author. Email: boris.landa@yale.edu

November 4, 2021

Abstract

Estimating the rank of a corrupted data matrix is an important task in data analysis, most notably for choosing the number of components in PCA. Significant progress on this task was achieved using random matrix theory by characterizing the spectral properties of large noise matrices. However, utilizing such tools is not straightforward when the data matrix consists of count random variables, e.g., Poisson, in which case the noise can be heteroskedastic with an unknown variance in each entry. In this work, we consider a Poisson random matrix with independent entries, and propose a simple procedure termed *biwhitening* for estimating the rank of the underlying signal matrix (i.e., the Poisson parameter matrix) without any prior knowledge. Our approach is based on the key observation that one can scale the rows and columns of the data matrix simultaneously so that the spectrum of the corresponding noise agrees with the standard Marchenko-Pastur (MP) law, justifying the use of the MP upper edge as a threshold for rank selection. Importantly, the required scaling factors can be estimated directly from the observations by solving a matrix scaling problem via the Sinkhorn-Knopp algorithm. Aside from the Poisson, our approach is extended to families of distributions that satisfy a quadratic relation between the mean and the variance, such as the generalized Poisson, binomial, negative binomial, gamma, and many others. This quadratic relation can also account for missing entries in the data. We conduct numerical experiments that corroborate our theoretical findings, and showcase the advantage of our approach for rank estimation in challenging regimes. Furthermore, we demonstrate the favorable performance of our approach on several real datasets of single-cell RNA sequencing (scRNA-seq), High-Throughput Chromosome Conformation Capture (Hi-C), and document topic modeling.

Keywords— rank estimation, PCA, heteroskedastic noise, Poisson noise, count data, Marchenko-Pastur law, rank selection, matrix scaling, Sinkhorn, bi-proportional scaling, scRNA-seq, Hi-C

1 Introduction

Principal Component Analysis (PCA) is a ubiquitous tool for processing and analyzing multivariate data [72, 40], and is widely used across multiple scientific fields for visualization, compression, denoising, and imputation. Yet, when applying PCA, one always faces the nontrivial task of setting the number of principal components that are retained for subsequent use. To address this challenge, a popular approach is to assume the signal-plus-noise model, which serves as a guidance for selecting the number of components in PCA. Specifically, let $Y \in \mathbb{R}^{m \times n}$ be a data matrix to be analyzed by PCA, and suppose that

$$Y = X + \mathcal{E}, \tag{1}$$

where X is a signal matrix with $\text{rank}\{X\} = r$, and \mathcal{E} is a noise matrix with $\mathbb{E}[\mathcal{E}_{i,j}] = 0$ for all $i \in [m]$ and $j \in [n]$. For simplicity of presentation we also assume that $m \leq n$, noting that one can always replace

Y with Y^T otherwise. Given the model above, we consider the task of estimating the rank r from the matrix of observations Y .

We mention that the literature on rank selection for PCA is vast – spanning several decades of research across multiple disciplines; see for instance [14, 71, 32, 60, 25, 16, 24, 43, 23, 36, 17, 47, 44] and references therein. In what follows, we only discuss lines of work that are relevant to our setting and approach.

1.1 Homoskedastic noise

It is well known that if the noise variables $\{\mathcal{E}_{i,j}\}_{i \in [m], j \in [n]}$ are i.i.d with variance σ^2 , namely, the noise is *homoskedastic*, then in the asymptotic regime of $m, n \rightarrow \infty$ and $m/n \rightarrow \gamma \in (0, 1]$, the spectrum of the noise matrix \mathcal{E} is described by the well-known Marchenko-Pastur law [55]. More precisely, letting $\Sigma = \frac{1}{n} \mathcal{E} \mathcal{E}^T$, we consider the *Empirical Spectral Distribution* (ESD) of the eigenvalues of Σ , defined by

$$F_{\Sigma}(\tau) = \frac{1}{m} \sum_{i=1}^m \mathbb{1}(\lambda_i\{\Sigma\} \leq \tau), \quad (2)$$

where $\mathbb{1}(\cdot)$ is the indicator function, and $\lambda_i\{\Sigma\}$ is the i 'th largest eigenvalue of Σ . Then, as $m, n \rightarrow \infty$ and $m/n \rightarrow \gamma \in (0, 1]$, the empirical spectral distribution $F_{\Sigma}(\tau)$ converges almost surely to the Marchenko-Pastur (MP) distribution $F_{\gamma, \sigma}(\tau)$ [55], which is the cumulative distribution function of the MP density

$$dF_{\gamma, \sigma}(\tau) = \frac{\sqrt{(\beta_+ - \tau)(\tau - \beta_-)}}{2\pi\sigma^2\gamma\tau} \mathbb{1}(\beta_- \leq \tau \leq \beta_+), \quad (3)$$

where $\beta_{\pm} = \sigma^2(1 \pm \sqrt{\gamma})^2$. A particular quantity of interest is the upper edge of the support of the MP density β_+ (also known as the upper bulk edge), primarily because the density of the eigenvalues beyond that point is 0. In fact, for many standard distributions for the noise entries $\mathcal{E}_{i,j}$ [26, 73], the spectrum of Σ satisfies the stronger property

$$\lambda_1\{\Sigma\} \xrightarrow{p} \beta_+, \quad (4)$$

where \xrightarrow{p} stands for convergence in probability (in the asymptotic regime $m, n \rightarrow \infty$, $m/n \rightarrow \gamma \in (0, 1]$).

We note that the spectral properties of Σ mentioned above are not restricted to the case of i.i.d noise variables [3], and also hold for noise matrices \mathcal{E} whose rows or columns were sampled independently from a random vector with mean zero and covariance $\sigma^2 I$ (where I is the identity matrix).

In the case of homoskedastic noise, a natural approach for estimating the rank r is by the number of eigenvalues of $n^{-1}YY^T$ that exceed the threshold $\sigma^2(1 + \sqrt{m/n})^2$, or equivalently, the number of singular values of Y that exceed $\sigma(\sqrt{m} + \sqrt{n})$. This approach has been extensively studied in the context of the spiked-model [4, 5, 6, 59, 61], which states that in the asymptotic regime of $m, n \rightarrow \infty$, $m/n \rightarrow \gamma \in (0, 1]$, and if the rank r and the singular values of X are fixed, each eigenvalue of $n^{-1}YY^T$ that is greater than β_+ corresponds to a nonzero eigenvalue of $n^{-1}XX^T$ (through a deterministic mapping), and the respective eigenvectors admit a nonzero correlation.

1.2 Heteroskedastic noise and count data

In many real-world applications the noise is not homoskedastic, and the noise variances can change arbitrarily across rows and columns. One notable example is count data, common in domains such as network traffic analysis [66], photon imaging [64], document topic modeling [70], Single-Cell RNA Sequencing (scRNA-seq) [30], and High-Throughput Chromosome Conformation Capture (Hi-C) [41], among many others (typically in the biological sciences). Specifically, let us consider a prototypical model where $\{Y_{i,j}\}_{i \in [m], j \in [n]}$ are independent with

$$Y_{i,j} \sim \text{Poisson}(X_{i,j}), \quad (5)$$

and $\{X_{i,j}\}$ are Poisson parameters (rates) satisfying $X_{i,j} > 0$. Since $\mathbb{E}[Y_{i,j}] = X_{i,j}$, the noise entries $\mathcal{E}_{i,j}$ from (1) are centered Poisson with variances $\mathbb{E}[\mathcal{E}_{i,j}^2] = X_{i,j}$.

Clearly, in the Poisson model (5) the noise variances $X_{i,j}$ can differ substantially, making the noise heteroskedastic in the most general sense. In this case, the MP law is not expected to hold, and the spectral distribution of the noise is determined by nonlinear equations known as the Dyson equations (see eq. (1.3) in [1]). These equations depend on the unknown variance profile of the noise. Hence, the limiting spectral distribution of the noise is nontrivial and is unavailable in advance, posing a major

challenge for rank estimation. Naturally, the same challenge arises for other distributions of $Y_{i,j}$ that admit a relation between the mean and the variance, such as for the binomial, negative binomial, gamma, and others (not necessarily count random variables).

A large portion of existing literature on PCA in heteroskedastic noise is dedicated to the task of estimating X or the subspaces spanning its rows and columns [35, 74, 34, 53, 51, 54, 12, 22]. However, in this line of work it is typically assumed that at least some information on the rank of X or on the noise variance profile is available (such as heteroskedasticity only across rows or across columns). Several recent works also considered the task of estimating X in the particular setting of count data [8, 63, 56, 13, 7], typically by solving a regularized optimization problem utilizing a low-rank model for X . Most recently, rank selection under heteroskedastic noise was considered in [36, 52, 45]. In particular, [52] provided an algorithm for computing the upper edge of the noise’s spectral distribution assuming that the noise variance profile is of rank one, [36] proposed a variant of parallel analysis that preserves the variance profile of the noise by random signflips, and [45] described a rank estimation procedure assuming a prior gamma distribution on the noise variances.

1.3 Our approach and contributions

In this work, we propose a new approach termed *biwhitening* for estimating the rank r in the Poisson model (5) (and other models) without requiring any prior knowledge on X or its spectrum. Our main idea is to guarantee that the standard MP law holds by applying appropriate diagonal scaling to Y , namely, multiplying its rows and columns by judiciously chosen scaling factors. These scaling factors can be estimated directly from the observation matrix Y , and their purpose is to make the average noise variance in each row and each column of the scaled noise matrix precisely 1. Then, we estimate r from the spectrum of the scaled version of Y as if the noise was homoskedastic with variance 1, that is, via the upper edge β_+ of the MP density $dF_{\gamma,1}$, taking $\gamma = m/n$. We derive our approach and justify it theoretically in the standard Poisson model (5), and further extend it to (almost) any distribution that satisfies a quadratic relation between the mean and the variance, i.e., $\text{Var}[Y_{i,j}] = a + bX_{i,j} + cX_{i,j}^2$, where $\text{Var}[Y_{i,j}]$ is the variance of $Y_{i,j}$ (the Poisson is a special case with $a = c = 0$, $b = 1$).

Our proposed biwhitening procedure for the Poisson model is described in Algorithm 1, where \mathbf{x} and \mathbf{y} are vectors of length m and n , respectively, $D(\mathbf{x})$ is a diagonal matrix with \mathbf{x} on its main diagonal, and $\mathbf{1}_m$ is a vector of m ones.

Algorithm 1 Biwhitening and rank estimation for Poisson data

Input: Nonnegative $m \times n$ Poisson count matrix Y .

- 1: Find positive vectors \mathbf{x} and \mathbf{y} so that $D(\mathbf{x})YD(\mathbf{y})$ has row sums $n \cdot \mathbf{1}_m$ and column sums $m \cdot \mathbf{1}_n$ by, e.g., the Sinkhorn-Knopp algorithm (see Algorithm 2 in Section 2.1).
 - 2: Form the biwhitened matrix $\hat{Y} = \sqrt{D(\mathbf{x})}Y\sqrt{D(\mathbf{y})}$.
 - 3: Estimate the rank r by the number of singular values of \hat{Y} that exceed $\sqrt{n} + \sqrt{m}$.
-

Figure 1 exemplifies the advantage of biwhitening on a simulated Poisson count matrix Y with $m = 300$, $n = 1000$, and $r = 10$. More details for reproducibility can be found in Appendix C.1. Notably, it is difficult to visually determine the true rank of X from the spectrum of Y , as the sorted eigenvalues of $n^{-1}YY^T$ admit a gradual decay and do not exhibit any significant gaps. Also, the histogram of these eigenvalues does not agree with the MP law (nor do we expect it to), and the MP upper edge β_+ does not provide an accurate threshold for determining the rank of X . On the other hand, once we apply biwhitening to Y , the rank $r = 10$ is “revealed” in the sense that the first r eigenvalues of $n^{-1}\hat{Y}\hat{Y}^T$ (where \hat{Y} is from Algorithm 1) are significantly separated from the rest of the spectrum – whose density agrees with the MP law, and whose upper edge is captured precisely by $\beta_+ = (1 + \sqrt{m/n})^2$.

The organization of this paper is as follows. In Section 2 we derive and analyze our approach in the Poisson model (5). In Section 3 we conduct numerical experiments that validate our theoretical results and demonstrate that our approach is robust to challenging regimes such as strong heteroskedasticity. In Section 4 we extend our approach to general families of distributions with quadratic variance functions and show that it can also account for missing entries in the data. In Section 5 we address important practical considerations such as adapting our approach to unknown data types, and exemplify our approach on several real datasets.

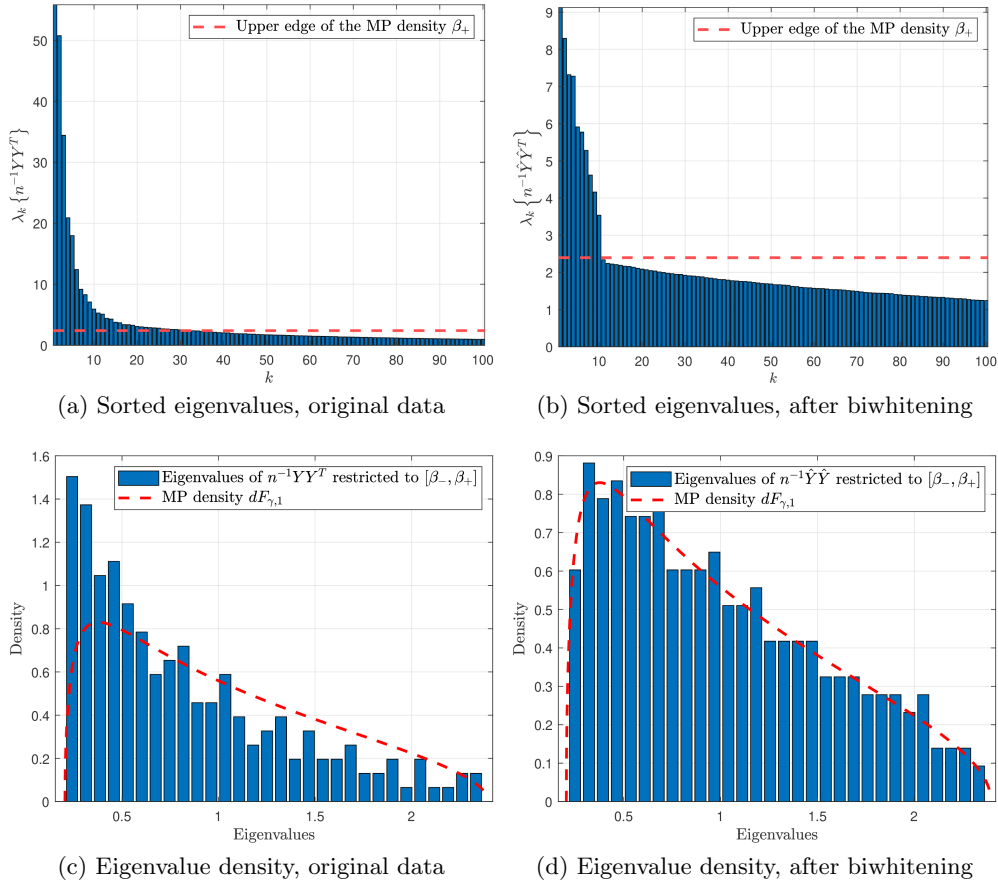


Figure 1: The spectrum of the original observation matrix and after applying biwhitening, for $m = 300$, $n = 1000$, and $r = 10$. The top two panels depict the sorted eigenvalues of $n^{-1}YY^T$ (top left) and $n^{-1}\hat{Y}\hat{Y}^T$ (top right) versus the upper edge β_+ of the MP density (dashed red line), where \hat{Y} is the biwhitened matrix from Algorithm 1. The bottom two panels depict the empirical density (i.e., normalized histogram) of the eigenvalues of $n^{-1}YY^T$ (bottom left) and $n^{-1}\hat{Y}\hat{Y}^T$ (bottom right) restricted to the support of the MP density, i.e., $[\beta_-, \beta_+]$, versus the MP density $dF_{\gamma,1}$ for $\gamma = m/n$ (dashed red line).

2 Method derivation and main results

2.1 Standardization of Poisson noise by diagonal scaling

The main idea underlying our approach is to appropriately scale the rows and columns of the Poisson matrix Y from (5), such that the noise component in the resulting scaled matrix satisfies the Marchenko-Pastur (MP) law (3). Towards that end, let $\mathbf{u} = [u_1, \dots, u_m]$ and $\mathbf{v} = [v_1, \dots, v_n]$ be positive vectors, and define

$$\tilde{Y} = D(\mathbf{u})YD(\mathbf{v}) = \tilde{X} + \tilde{\mathcal{E}}, \quad (6)$$

where Y is from (5), $D(\mathbf{u})$ and $D(\mathbf{v})$ are diagonal matrices with \mathbf{u} and \mathbf{v} on their main diagonals, respectively, and

$$\tilde{X} = D(\mathbf{u})XD(\mathbf{v}), \quad \tilde{\mathcal{E}} = D(\mathbf{u})\mathcal{E}D(\mathbf{v}). \quad (7)$$

Notably, $\tilde{\mathcal{E}}$ and \tilde{X} preserve several important properties of the noise matrix \mathcal{E} and the signal matrix X . In particular, the scaled noise random variables $\{\tilde{\mathcal{E}}_{i,j}\} = \{u_i\mathcal{E}_{i,j}v_j\}$ are independent with zero means, and

$$\text{Rank}\{\tilde{X}\} = \text{Rank}\{D(\mathbf{u})XD(\mathbf{v})\} = \text{Rank}\{X\} = r, \quad (8)$$

since diagonal scaling (with nonzero scaling factors) preserves the row and column spaces of a matrix. Hence, we can translate the task of estimating the rank of X to the analogous task of estimating the rank

of \tilde{X} . Crucially, the diagonal scaling in (6) allows us to control certain aspects of the variance profile of the scaled noise matrix $\tilde{\mathcal{E}}$. While we cannot use this diagonal scaling to make all the (entrywise) variances $\mathbb{E}[\tilde{\mathcal{E}}_{i,j}^2]$ equal (unless X is of rank 1), we use \mathbf{u} and \mathbf{v} that enforce the average variance in each row and each column of $\tilde{\mathcal{E}}$ to be 1. Specifically, we consider \mathbf{u} and \mathbf{v} that satisfy

$$1 = \frac{1}{m} \sum_{i=1}^m \mathbb{E}[\tilde{\mathcal{E}}_{i,j}^2] = \frac{1}{m} \sum_{i=1}^m u_i^2 X_{i,j} v_j^2, \quad \text{and} \quad 1 = \frac{1}{n} \sum_{j=1}^n \mathbb{E}[\tilde{\mathcal{E}}_{i,j}^2] = \frac{1}{n} \sum_{j=1}^n u_i^2 X_{i,j} v_j^2, \quad (9)$$

for all $i \in [m]$ and $j \in [n]$, using the fact that $\mathbb{E}[\mathcal{E}_{i,j}^2] = X_{i,j}$ in the Poisson model (1). It is worthwhile to point out that since $\{\tilde{\mathcal{E}}_{i,j}\}$ are independent and have zero means, the equations in (9) are equivalent to

$$\mathbb{E}\left[\frac{1}{n} \tilde{\mathcal{E}} \tilde{\mathcal{E}}^T\right] = I_m, \quad \text{and} \quad \mathbb{E}\left[\frac{1}{m} \tilde{\mathcal{E}}^T \tilde{\mathcal{E}}\right] = I_n, \quad (10)$$

where I_m and I_n are the $m \times m$ and $n \times n$ identity matrices, respectively. Observe that (10) is satisfied by typical homoskedastic noise models. In particular, (10) holds if we replace $\tilde{\mathcal{E}}$ by any matrix whose entries are independent with mean zero and variance one, and more generally, if we replace $\tilde{\mathcal{E}}$ by a matrix whose either rows or columns are sampled independently from an isotropic random vector (i.e., a random vector whose mean is zero and covariance is the identity matrix). Indeed, Equation (10) is the motivation for the name *biwhitening*.

Since \mathbf{u} and \mathbf{v} from (9) are the solution to a nonlinear system of equations, it may not be immediately obvious that such a solution exists, whether or not it is unique, and how to find it. These questions can be settled by observing that (9) is in fact an instance of a problem known as *matrix scaling* (also *matrix balancing* or *bi-proportional scaling*); see [39] for an extensive review of the topic. Specifically, given a nonnegative matrix $A \in \mathbb{R}^{m \times n}$ and positive vectors $\mathbf{r} = [r_1, \dots, r_m]$ and $\mathbf{c} = [c_1, \dots, c_n]$, the goal in matrix scaling is to find positive vectors $\mathbf{x} = [x_1, \dots, x_m]$ and $\mathbf{y} = [y_1, \dots, y_n]$ such that the matrix $D(\mathbf{x})AD(\mathbf{y})$ has prescribed row sums \mathbf{r} and column sums \mathbf{c} , i.e.,

$$c_j = \sum_{i=1}^m x_i A_{i,j} y_j, \quad \text{and} \quad r_i = \sum_{j=1}^n x_i A_{i,j} y_j, \quad (11)$$

for all $i \in [m]$ and $j \in [n]$. We will refer to positive \mathbf{x} and \mathbf{y} that solve (11) as *scaling factors* of A , and say that \mathbf{x} and \mathbf{y} scale A to row sums \mathbf{r} and column sums \mathbf{c} . Clearly, the equations in (9) are equivalent to those in (11) if we take $A = X$, $r_i = n$, $c_j = m$, $x_i = u_i^2$, and $y_j = v_j^2$.

When the scaling factors of A exist, they can be found by the Sinkhorn-Knopp algorithm [69, 62]; see Algorithm 2. For the convergence rate of the Sinkhorn-Knopp algorithm, see [46, 2, 15] and references therein. As for the existence and uniqueness of the scaling factors, the subject has been extensively studied [67, 68, 11, 10, 19]. In particular, we have the following proposition for the system of equations in (9).

Proposition 1 (Existence and uniqueness of \mathbf{u} and \mathbf{v}). *There exists a pair (\mathbf{u}, \mathbf{v}) of positive vectors that satisfies (9) for all $i \in [m]$ and $j \in [n]$. Furthermore, (\mathbf{u}, \mathbf{v}) is unique up to a positive scalar, namely it can only be replaced with $(a\mathbf{u}, a^{-1}\mathbf{v})$ for any $a > 0$.*

The proof follows immediately from Theorem 1 in [67] when taking $A = X$, $r_i = n$, $c_j = m$, $x_i = u_i^2$, and $y_j = v_j^2$, using the fact that X is strictly positive and $\sum_{i=1}^m r_i = mn = \sum_{j=1}^n c_j$.

According to Proposition 1, the products $\{u_i v_j\}_{i \in [m], j \in [n]}$ are determined uniquely by X , which means that the scaled noise matrix $\tilde{\mathcal{E}} = (\mathcal{E}_{i,j} u_i v_j)_{i \in [m], j \in [n]}$ is a random matrix also uniquely determined by X . It is then of interest to characterize the spectral properties of $\tilde{\mathcal{E}}$, particularly in the regime of large m and n , noting that the singular values of $\tilde{\mathcal{E}}$ can be directly obtained from the eigenvalues of the matrix $\tilde{\Sigma} = n^{-1} \tilde{\mathcal{E}} (\tilde{\mathcal{E}})^T$. To characterize the spectral behavior of $\tilde{\mathcal{E}}$, let $\{m_n\}_{n \geq 1}$ be a sequence of positive integers such that $m_n \xrightarrow{n \rightarrow \infty} \infty$ and $m_n/n \xrightarrow{n \rightarrow \infty} \gamma \in (0, 1]$. In addition, let $\{X^{(n)}\}_{n \geq 1}$ and $\{\tilde{\mathcal{E}}^{(n)}\}_{n \geq 1}$ be sequence of $m_n \times n$ matrices defined equivalently to X and $\tilde{\mathcal{E}}$, respectively, and define $\tilde{\Sigma}^{(n)} = n^{-1} \tilde{\mathcal{E}}^{(n)} (\tilde{\mathcal{E}}^{(n)})^T$. We then have the following result.

Theorem 2 (Marchenko-Pastur law and the limit of the largest eigenvalue of $\tilde{\Sigma}^{(n)}$). *Suppose that there exist universal constants $C, c > 0$ such that $c \leq \max_{i,j} X_{i,j}^{(n)} \leq C \min_{i,j} X_{i,j}^{(n)}$ for all $i \in [m]$, $j \in [n]$, and $n \geq 1$. Then, as $n \rightarrow \infty$, the empirical spectral distribution of $\tilde{\Sigma}^{(n)}$, given by $F_{\tilde{\Sigma}^{(n)}}$ (see (2)), converges almost surely to the Marchenko-Pastur distribution with parameter γ and noise variance $\sigma^2 = 1$, i.e., $F_{\gamma,1}$. Furthermore, we have that $\lambda_1\{\tilde{\Sigma}^{(n)}\} \xrightarrow{p} \beta_+ = (1 + \sqrt{\gamma})^2$.*

Algorithm 2 The Sinkhorn-Knopp algorithm

- Input:** Nonnegative $m \times n$ matrix A , prescribed row sums \mathbf{r} and column sums \mathbf{c} , tolerance $\delta > 0$.
- 1: Initialize: $\mathbf{x}^{(0)} = \mathbf{1}_m$, $\mathbf{y}^{(0)} = \mathbf{1}_n$, $\tau = 0$.
 - 2: While $\max_{i \in [m]} |\sum_{j=1}^n x_i^{(\tau)} A_{i,j} y_j^{(\tau)} - r_i| > \delta$ or $\max_{j \in [n]} |\sum_{i=1}^m x_i^{(\tau)} A_{i,j} y_j^{(\tau)} - c_j| > \delta$, do:
 - $\mathbf{y}_j^{(\tau+1)} = c_j / (\sum_{i=1}^m A_{i,j} x_i^{(\tau)})$, for $j = 1, \dots, n$.
 - $\mathbf{x}_i^{(\tau+1)} = r_i / (\sum_{j=1}^n A_{i,j} y_j^{(\tau+1)})$, for $i = 1, \dots, m$.
 - Update $\tau \leftarrow \tau + 1$.
 - 3: Return $\mathbf{x}^{(\tau)}$ and $\mathbf{y}^{(\tau)}$.
-

Essentially, under the conditions in Theorem 2 and in the asymptotic regime of $m, n \rightarrow \infty$, $m/n \rightarrow \gamma \in (0, 1]$, the spectrum of the noise $\tilde{\mathcal{E}}$ behaves as if the noise was homoskedastic, namely that the MP law holds and the largest eigenvalue of $\tilde{\Sigma}$ converges to the upper edge of the MP bulk β_+ (see Section 1.1). The condition $c < \max_{i,j} X_{i,j}^{(n)} \leq C \min_{i,j} X_{i,j}^{(n)}$ in Theorem 2 requires that the Poisson parameters $X_{i,j}^{(n)}$ are always bounded away from zero, and that all of them admit the same growth rate with n (i.e., none of the Poisson parameters can grow unbounded with n relative to others). Even with this restriction, the ratios $X_{i,j}^{(n)} / X_{k,\ell}^{(n)}$ for $(i,j) \neq (k,\ell)$ can vary, and can be very large or very small for certain pairs (i,j) and (k,ℓ) , allowing for substantial heteroskedasticity of the noise in the model (1). The proof of Theorem 2 can be found in Appendix F, and relies on the results of [27] and [1] with certain boundedness properties of the scaling factors \mathbf{u} and \mathbf{v} .

Next, using the fact that $\text{rank}\{\tilde{X}\} = \text{rank}\{X\}$ and $\lambda_1\{\tilde{\Sigma}^{(n)}\} \xrightarrow{p} (1 + \sqrt{\gamma})^2$, it is natural to consider the following estimator for the rank r of X :

$$\tilde{r}_\varepsilon = \max \left\{ k : \lambda_k \{n^{-1} \tilde{Y} \tilde{Y}^T\} > \left(1 + \sqrt{\frac{m}{n}}\right)^2 + \varepsilon \right\}, \quad (12)$$

where $\varepsilon > 0$ and $\lambda_k \{n^{-1} \tilde{Y} \tilde{Y}^T\}$ is the k 'th largest eigenvalue of $n^{-1} \tilde{Y} \tilde{Y}^T$. In words, we take \tilde{r}_ε to be the number of eigenvalues of $n^{-1} \tilde{Y} \tilde{Y}^T$ that are not included in the ε -neighborhood of the Marchenko-Pastur bulk. Let us consider again the asymptotic setting of $m_n \rightarrow \infty$, $m_n/n \rightarrow \gamma \in (0, 1]$, letting $\text{rank}\{X^{(n)}\} = r^{(n)} < m_n$, and $\tilde{r}_\varepsilon^{(n)}$ be as \tilde{r}_ε from (12) when replacing \tilde{Y} with $\tilde{Y}^{(n)}$. We then have the following property of the rank estimator $\tilde{r}_\varepsilon^{(n)}$ in the asymptotic regime of $n \rightarrow \infty$.

Theorem 3. *Under the conditions in Theorem 2, $\Pr\{r^{(n)} < \tilde{r}_\varepsilon^{(n)}\} \xrightarrow[n \rightarrow \infty]{} 0$ for any $\varepsilon > 0$.*

The proof can be found in Appendix G, and relies on Theorem 2 and the fact that diagonal scaling preserves the rank of X (see (8)). Fundamentally, Theorem 3 states that in the asymptotic setting of $m, n \rightarrow \infty$, $m/n \rightarrow \gamma \in (0, 1]$, the rank estimator \tilde{r}_ε does not overestimate the rank of X for any $\varepsilon > 0$ (with probability approaching 1). Taking $\varepsilon \rightarrow 0$, this result implies that for sufficiently large m and n , all eigenvalues of $n^{-1} \tilde{Y} \tilde{Y}^T$ that exceed $(1 + \sqrt{m/n})^2$ by an arbitrarily-small positive value correspond to true signal components, i.e., to nonzero singular values of X . The reason that (12) asymptotically underestimates the rank is that some of the signal components can be too weak for detection. In particular, the existence of small eigenvalues of $n^{-1} \tilde{X} \tilde{X}^T$ can be masked by the bulk of the eigenvalues of the noise $n^{-1} \tilde{\mathcal{E}} \tilde{\mathcal{E}}^T$ (given by the MP distribution); see [4, 5, 6, 59, 61] for more details on this phenomenon in the case of homoskedastic noise and the spiked-model (noting that our model does not require the rank of $X^{(n)}$ to be fixed).

2.2 Estimating the scaling factors \mathbf{u} and \mathbf{v}

The immediate obstacle in employing \mathbf{u} and \mathbf{v} that satisfy (9) is that $\{X_{i,j}\}_{i \in [m], j \in [n]}$ are unknown. Nonetheless, while we do not have access to $X_{i,j}$, we do have access to an unbiased estimator of $X_{i,j}$, which is $Y_{i,j}$. Therefore, instead of solving (9), we propose to find positive vectors $\hat{\mathbf{u}} = [\hat{u}_1, \dots, \hat{u}_m]$ and $\hat{\mathbf{v}} = [\hat{v}_1, \dots, \hat{v}_n]$ that solve the surrogate system of equations obtained by replacing $X_{i,j}$ in (9) with $Y_{i,j}$,

i.e.,

$$1 = \frac{1}{m} \sum_{i=1}^m \hat{u}_i^2 Y_{i,j} \hat{v}_j^2, \quad \text{and} \quad 1 = \frac{1}{n} \sum_{j=1}^n \hat{u}_i^2 Y_{i,j} \hat{v}_j^2, \quad (13)$$

for all $i \in [m]$ and $j \in [n]$. Analogously to (6), we then define

$$\hat{Y} = D(\hat{\mathbf{u}})YD(\hat{\mathbf{v}}) = \hat{X} + \hat{\mathcal{E}}, \quad (14)$$

where $\hat{X} = D(\hat{\mathbf{u}})XD(\hat{\mathbf{v}})$, $\hat{\mathcal{E}} = D(\hat{\mathbf{u}})\mathcal{E}D(\hat{\mathbf{v}})$, and equivalently to (8) we have $\text{Rank}\{\hat{X}\} = \text{Rank}\{X\} = r$. Similarly to (9), the system of equations in (13) is an instance of (11) if we set $A = Y$, $r_i = n$, $c_j = m$, $x_i = \hat{u}_i^2$, and $y_j = \hat{v}_j^2$.

It is important to note that in contrast to the matrix X in (9), a realization of the random matrix Y may not be strictly positive and may contain zeros, hence the existence and uniqueness of positive $\hat{\mathbf{u}}$ and $\hat{\mathbf{v}}$ that satisfy (13) is not obvious. Indeed, in the most general case of matrix scaling, the existence and uniqueness of \mathbf{x} and \mathbf{y} that satisfy (11) depends on the particular zero pattern of A (i.e., the set of indices (i, j) for which $A_{i,j} = 0$); see the end of this section and Appendix A for more details.

Let us consider again the asymptotic setting where $\{m_n\}_{n \geq 1}$ is a sequence of positive integers such that $m_n \xrightarrow{n \rightarrow \infty} \infty$ and $m_n/n \xrightarrow{n \rightarrow \infty} \gamma \in (0, 1]$, and let $(\mathbf{u}^{(n)}, \mathbf{v}^{(n)})$ be the solution to (9) corresponding to $X^{(n)} \in \mathbb{R}^{m_n \times n}$ (replacing X) and satisfying $\|\mathbf{u}^{(n)}\|_2 = \|\mathbf{v}^{(n)}\|_2$ (such a solution exists and is unique according to Proposition 1). In addition, let $\{Y^{(n)}\}_{n \geq 1}$ be a sequence of $m_n \times n$ random matrices with independent Poisson entries (analogous to Y) such that $\mathbb{E}[Y^{(n)}] = X^{(n)}$, and define $\hat{\mathbf{u}}^{(n)}$ and $\hat{\mathbf{v}}^{(n)}$ analogously to $\hat{\mathbf{u}}$ and $\hat{\mathbf{v}}$, respectively, when replacing Y in (13) with $Y^{(n)}$. We now provide the following result.

Lemma 4 (Convergence of estimated scaling factors). *Suppose that there exist universal constants $C, c, \epsilon > 0$ such that $c(\log n)^{1+\epsilon} \leq \max_{i,j} X_{i,j}^{(n)} \leq C \min_{i,j} X_{i,j}^{(n)}$ for all $i \in [m]$, $j \in [n]$, and $n \geq 1$. Then, there is a constant $\tilde{C} > 0$ such that with probability that tends to 1 as $n \rightarrow \infty$, there exists a pair of positive scaling factors $(\hat{u}^{(n)}, \hat{v}^{(n)})$ that solves (13) and a scalar $a_n > 0$, which satisfy*

$$\left| \frac{a_n \hat{u}_i^{(n)}}{u_i^{(n)}} - 1 \right| \leq \tilde{C} \sqrt{\frac{\log n}{n}}, \quad \left| \frac{a_n^{-1} \hat{v}_j^{(n)}}{v_j^{(n)}} - 1 \right| \leq \tilde{C} \sqrt{\frac{\log n}{n}}, \quad (15)$$

for all $i \in [m]$ and $j \in [n]$.

The proof of Lemma 4 can be found in Appendix H, and relies on the results in [48]. Note that the convergence of the estimated scaling factors $(\hat{\mathbf{u}}, \hat{\mathbf{v}})$ to the true scaling factors (\mathbf{u}, \mathbf{v}) in Lemma 4 is up to an arbitrary sequence of positive scalars $\{a_n\}$, which arise from the fundamental ambiguity in the uniqueness of the scaling factors; see Proposition 1. We note that the statement in Lemma 4 is particularly useful for our subsequent analysis and is more informative for our purposes than a statement on the convergence rate of the errors $|\hat{u}_i^{(n)} \hat{v}_j^{(n)} - u_i^{(n)} v_j^{(n)}|$ (which do not involve the arbitrary scalars $\{a_n\}$).

Let us define $\hat{\Sigma}^{(n)} = n^{-1} \hat{\mathcal{E}}^{(n)} (\hat{\mathcal{E}}^{(n)})^T$. Using Lemma 4 we obtain the following result, which establishes the convergence of the spectrum of $\hat{\Sigma}^{(n)}$ to the spectrum of $\tilde{\Sigma}^{(n)}$ in probability as $n \rightarrow \infty$.

Theorem 5 (Spectral convergence of $\hat{\Sigma}^{(n)}$ to $\tilde{\Sigma}^{(n)}$). *Suppose that the conditions in Lemma 4 hold. Then, $\max_{i \in [m_n]} |\lambda_i\{\hat{\Sigma}^{(n)}\} - \lambda_i\{\tilde{\Sigma}^{(n)}\}| \xrightarrow{P} 0$.*

The proof can be found in Appendix I. We mention that the main difference between the conditions in Theorem 2 and those in Theorem 5 is that we further impose a growth rate – slightly larger than logarithmic – on the Poisson parameters $X_{i,j}$, namely the condition $(c/C)(\log n)^{1+\epsilon} \leq \min_{i,j} X_{i,j}^{(n)}$ for some $\epsilon > 0$. Notably, this condition guarantees that the observation matrix $Y^{(n)}$ is strictly positive with probability approaching 1 as $n \rightarrow \infty$ (using the fact that $\Pr\{Y_{i,j}^{(n)} = 0\} = \exp(-X_{i,j}^{(n)})$, which together with the union bound gives $\Pr\{\cup_{i,j} \{Y_{i,j}^{(n)} = 0\}\} \leq m_n n \exp(-X_{i,j}^{(n)}) \xrightarrow{n \rightarrow \infty} 0$, in the asymptotic regime $m_n, n \rightarrow \infty$, $m_n/n \rightarrow \gamma$). Although our analysis here is concerned with an asymptotically positive realization of the random matrix Y , the numerical experiments in Section 3.1 demonstrate that our results also hold when a realization of Y can contain zeros.

Under the conditions in Lemma 4 and by combining Theorems 2 and 5, we get that the empirical spectral distribution of $\hat{\Sigma}^{(n)}$ converges to the MP distribution $F_{\gamma,1}$, and furthermore, $\lambda_1\{\hat{\Sigma}^{(n)}\} \xrightarrow{P}$

$(1 + \sqrt{\gamma})^2$. Consequently, we propose to estimate r from \hat{Y} analogously to (12) by replacing Y with \hat{Y} . We mention that an analogous version of Theorem 3 can be proved for this estimator by repeating the proof of Theorem 3 and making use of Theorems 2 and 5.

Recall that the equations for $\hat{\mathbf{u}}$ and $\hat{\mathbf{v}}$ in (13) are equivalent to the equations in (11) for \mathbf{x} and \mathbf{y} when taking $A = Y$, $x_i = \hat{u}_i^2$, $y_j = \hat{v}_j^2$, $r_i = n$, and $c_j = m$. Since a realization of the random matrix Y may contain zeros, it is important to understand under which circumstances we have existence and uniqueness of positive \mathbf{x} and \mathbf{y} that satisfy (11) for $r_i = n$ and $c_j = m$, where A is a deterministic nonnegative matrix that represents a realization of Y with zeros. We provide a comprehensive review of this topic in Appendix A, and derive the following simple guarantee on the existence and uniqueness of \mathbf{x} and \mathbf{y} in terms of the zeros in A .

Proposition 6 (Existence and uniqueness of \mathbf{x} and \mathbf{y} for $r_i = n$, $c_j = m$). *Let $r_i = n$ and $c_j = m$ for all $i \in [m]$ and $j \in [n]$ in (11). Suppose that A does not have any zero rows and columns, and that both requirements below are met:*

1. For each $k = 1, 2, \dots, \lfloor n/2 \rfloor$, A has less than $\lceil mk/n \rceil$ rows that have at least $n - k$ zeros each.
2. For each $\ell = 1, 2, \dots, \lfloor m/2 \rfloor$, A has less than $\lceil n\ell/m \rceil$ columns that have at least $m - \ell$ zeros each.

Then, there exists a pair (\mathbf{x}, \mathbf{y}) of positive vectors that satisfies (11), and it is unique up to a positive scalar, namely it can only be replaced with $(a\mathbf{x}, a^{-1}\mathbf{y})$ for any $a > 0$.

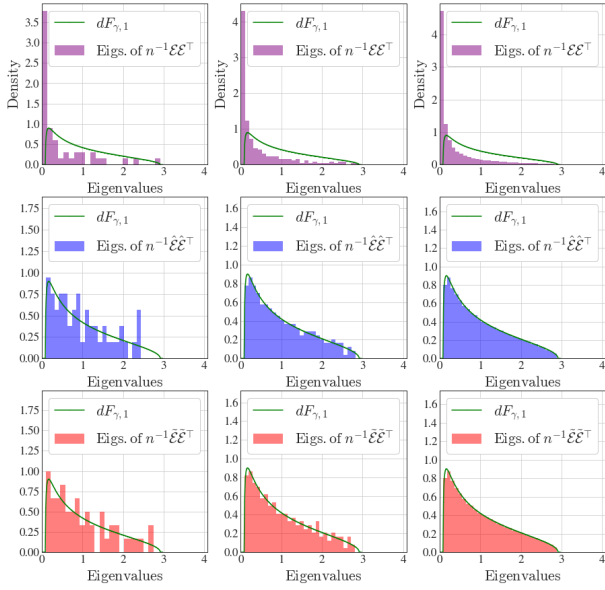
Observe that the conditions in Proposition 6 are only concerned with rows or columns of A that have at least $\lceil m/2 \rceil$ and $\lceil n/2 \rceil$ zeros, respectively. Therefore, the existence and uniqueness guarantees in Proposition 6 hold if the majority of entries in each row and each column of A are positive. Aside from this simple sufficient condition for existence and uniqueness, Proposition 6 also allows A to have a small number of rows and columns in which all but a few entries are zero, and moreover, A can potentially have a large number of rows or columns with more than half their entries being zero. See Appendix A for more details on the existence and uniqueness of \mathbf{x} and \mathbf{y} , and on appropriate preprocessing steps that can be taken to guarantee them.

3 Experiments on simulated Poisson data

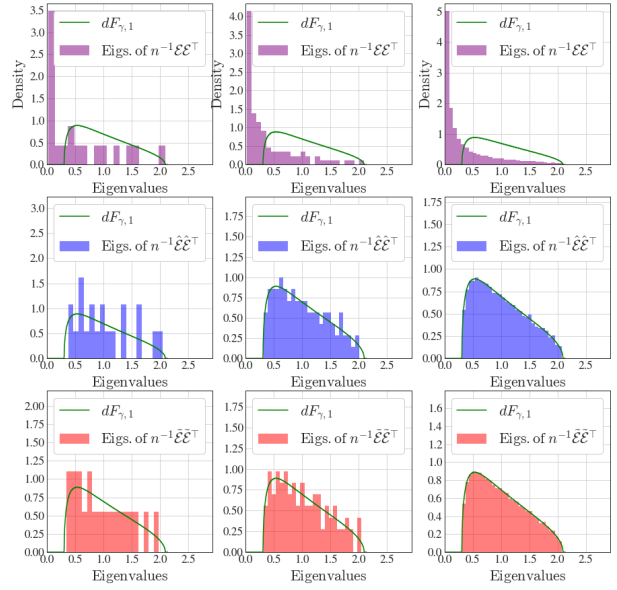
3.1 Fit against the MP law

We begin by measuring how well our proposed scaling of Poisson noise fits the theoretical MP law with $\sigma = 1$ (see Theorem 2), and compare it against the empirical eigenvalue density of the original noise matrix (without any scaling). In Figure 2 we illustrate the eigenvalue histograms (normalized appropriately) for the matrices $\Sigma_n = n^{-1}YY^T$, $\hat{\Sigma}_n = n^{-1}\hat{Y}\hat{Y}^T$, and $\tilde{\Sigma}_n = n^{-1}\tilde{Y}\tilde{Y}^T$, using the aspect ratios $\gamma = m/n = 1/2, 1/5$ and increasing dimension $n = 100, 500, 5000$. For visualization purposes, we normalized Σ_n by a scalar so that its largest eigenvalue is the MP law upper edge $(1 + \sqrt{\gamma})^2$ (for $\sigma = 1$). More details for reproducibility can be found in Appendix C.2. We observe that while the eigenvalue histogram for the original noise (i.e., without any scaling) is very different from the MP law, there is a good fit between the MP law and the eigenvalue histogram of the noise after scaling (using either the exact or the estimated scaling factor) which clearly improves upon increasing matrix dimensions. The analogous results for the aspect ratios $\gamma = m/n = 1/3, 1/4$ can be found in Figure 7 in Appendix B

In Figure 3, we visualize the Kolmogorov-Smirnov (KS) distances (see [29]) $\sup_x \mathbb{E} \left[|F_{\tilde{\Sigma}_n}(x) - F_{\gamma,1}(x)| \right]$ (red curve) and $\sup_x \mathbb{E} \left[|F_{\hat{\Sigma}_n}(x) - F_{\gamma,1}(x)| \right]$ (blue curve) as functions of the dimension n , where $F_{\tilde{\Sigma}_n}$ and $F_{\hat{\Sigma}_n}$ are the empirical spectral distributions (see (2)) of $\tilde{\Sigma}_n$ and $\hat{\Sigma}_n$, respectively, and $F_{\gamma,1}$ is the MP distribution with $\sigma = 1$. For this figure, we simulated Y in the same way as we did for Figure 2, and averaged the KS distance over 20 randomized experiments. As expected from the analysis in Section 2, we see that the empirical spectral distribution of the scaled noise matrix converges to the MP law, using either the exact or the estimated scaling factors. It is important to mention that even though Theorem 5 requires the Poisson parameters $X_{i,j}$ to increase with (slightly larger than a) logarithmic rate with n , the convergence to the MP law in this experiment is achieved without this condition (as the Poisson parameters in this experiment are upper bounded).

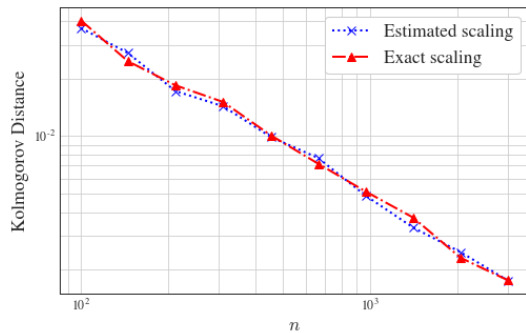


(a) $\gamma = 1/2$, $n = 100, 500, 5000$

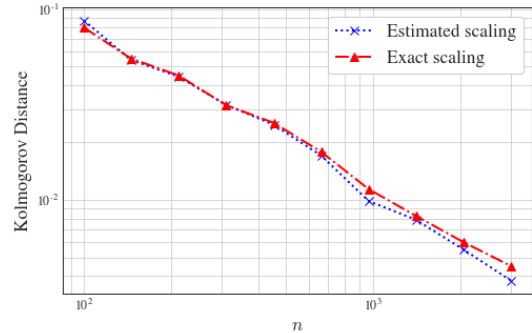


(b) $\gamma = 1/5$, $n = 100, 500, 5000$

Figure 2: Spectrum of simulated Poisson noise versus the standard ($\sigma = 1$) Marchenko-Pastur density $dF_{\gamma,1}$, for various aspect ratios γ and matrix dimensions $n = 100, 500, 5000$ (from left to right in each panel). The top row in each panel (purple) is the histogram of the eigenvalues of Σ_n (i.e., without any row or column scaling). The center row in each panel (blue) is the histogram of the eigenvalues of $\hat{\Sigma}_n$ (i.e., after scaling with the estimated scaling factors). The bottom row in each panel (red) is the histogram of eigenvalues of $\tilde{\Sigma}_n$ (i.e., after scaling with the exact scaling factors).



(a) $\gamma = 1/2$



(b) $\gamma = 1/5$

Figure 3: Convergence of the empirical spectral distribution (see (2)) of $\tilde{\Sigma}_n$ (true scaling - red curve) and the empirical spectral distribution of $\hat{\Sigma}_n$ (estimated scaling - blue curve) to the MP distribution $F_{\gamma,1}$, as the column dimension n increases.

3.2 Rank estimation accuracy

Next, we demonstrate the accuracy of Algorithm 1 for rank estimation under various degrees of heteroskedasticity, and compare it to several other methods: the Empirical Kaiser Criterion (EKC) [9], pairwise Parallel Analysis (PA) (see Algorithm 1 in [21]), Deflated Deterministic Parallel Analysis+ (DDPA+) [21], and Signflip Parallel Analysis (Signflip PA) [36]. For DDPA+, we input the column-wise centered matrix, where each column has its mean subtracted from it. For Signflip PA, we input the column-wise centered matrix whose rows are further normalized (i.e., each row is divided by its Euclidean norm), as suggested in [36] in their experiments. We found empirically that these preprocessing steps are essential for these methods to select a nontrivial rank (beyond 1) in the settings of our experiments.

We performed three experiments, each one simulating a different scenario. In each one, we generated a matrix X of Poisson parameters in a different way, where the rank is always 20 and the dimensions are $m = 500$, $n = 750$. In the first experiment, we generated a matrix X with little variation in the magnitudes of the entries across rows or columns, facilitating a vanilla scenario of mild heteroskedasticity. In the second experiment, we generated a matrix X with substantial variation in the magnitudes of the entries across rows or columns, corresponding to a challenging regime of strong heteroskedasticity. Lastly, in the third experiment we generated a matrix X such that one of the 20 signal components is much stronger than the rest (the noise is also heteroskedastic due to variation in the entries of the strong factor). This last regime is particularly challenging for methods based on Monte-Carlo simulations (PA, Signflip PA) due to *shadowing* [20] – a phenomenon where strong signal components introduce bias into the estimation of the spectrum of the noise. More details on the simulation of our different settings can be found in Appendix C.3. After generating X for each experiment, we normalized X (excluding the strong factor in the third experiment) so that its average Poisson parameter has a prescribed value that serves as an average signal-to-noise ratio. We then report the rank estimated by the different methods for a wide range of average Poisson parameter values. In Figure 4 we plot the estimated ranks when averaged over 20 randomized trials, as well as and their $[0.1, 0.9]$ quantiles, as a function of the average Poisson parameter in the matrix.

In the first scenario (Figure 4a), where the heteroskedasticity is mild, it is evident that all methods perform similarly. In particular, when the Poisson parameters are small, the signal eigenvalues are not large enough to be detected, hence the ranks estimated by all methods are 1. Then, as the average Poisson parameter grows, more and more signal eigenvalues become large enough to be detected, and the estimated ranks (by all methods) gradually increase until they stabilize at the correct rank of 20. Even in this easy setting, our method and the EKC perform slightly better than the other methods, allowing for accurate rank estimation for smaller Poisson parameters (lower signal-to-noise ratios). Intuitively, the reason for this is that both our method and the EKC perform a normalization that stabilizes the noise variances (explicitly in our method and implicitly in the EKC), which controls the spectrum of the noise and restricts its large eigenvalues from being dominated by rows/columns with larger noise variances.

In the second and third scenarios (Figures 4b and 4c), which are more challenging, the performance of the other methods substantially degrades. In particular, the methods that were not designed to handle heteroskedastic noise (all methods except ours and Signflip PA) perform poorly in the second scenario, and the methods that are based on simulations (PA, Signflip PA) perform poorly in the third scenario. DDPA+ can occasionally detect the correct rank in the third scenario (as it is designed to cope with strong signal factors by subtracting them), but its behavior is unstable due to the heteroskedastic noise. Evidently, our method is the only one that converges to the correct rank in a stable manner across all scenarios, and is able to detect the correct rank with smaller Poisson parameters (lower signal-to-noise ratios).

4 Beyond the Poisson distribution

Let us consider the model (1) where $Y_{i,j}$ are independent but not necessarily Poisson, $X = \mathbb{E}[Y]$ is the matrix whose rank is of interest, and $\mathcal{E} = Y - \mathbb{E}[Y]$ is the corresponding noise matrix. Recall that the main idea underlying our approach is to diagonally scale the data matrix Y to $D(\mathbf{u})YD(\mathbf{v})$, so that the average variance in each row and in each column of the scaled noise matrix $D(\mathbf{u})\mathcal{E}D(\mathbf{v})$ is 1. Therefore, analogously to (9), we consider positive \mathbf{u} and \mathbf{v} that satisfy

$$1 = \frac{1}{m} \sum_{i=1}^m u_i^2 \text{Var}[Y_{i,j}] v_j^2, \quad \text{and} \quad 1 = \frac{1}{n} \sum_{j=1}^n u_i^2 \text{Var}[Y_{i,j}] v_j^2, \quad (16)$$

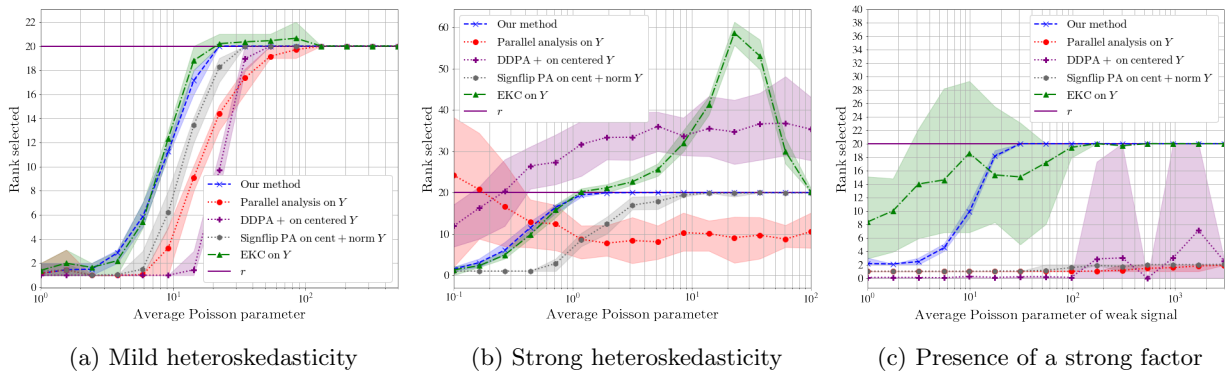


Figure 4: Rank selection accuracy of several methods, as well as their variability ([0.1, 0.9] quantile range depicted as the shaded areas), for a Poisson count matrix generated from X with rank $r = 20$, $m = 500$, and $n = 750$. On the x-axis, we have the average Poisson parameter in the matrix, while on the y-axis, we have the ranks determined by the algorithms. In the leftmost figure, the Poisson parameter matrix is generated to be relatively uniform, such that the noise is only mildly heteroskedastic. In the center figure, we demonstrate the impact of heteroskedasticity by substantially increasing the variability of the parameter matrix across rows and columns. In the rightmost figure, we consider the impact of having a strong signal component.

for all $i \in [m]$ and $j \in [n]$, where $\text{Var}[Y_{i,j}]$ is the variance of $Y_{i,j}$. Equivalently to Proposition 1, if all the variances $\text{Var}[Y_{i,j}]$ are strictly positive, then positive \mathbf{u} and \mathbf{v} that satisfy (16) are guaranteed to exist and are unique up to a positive scalar.

Under appropriate conditions on the variances of $\{\mathcal{E}_{i,j}\}$ and their higher order moments, Theorem 2 can be trivially extended to account for distributions of $Y_{i,j}$ other than the Poisson. In particular, we have the following proposition, which provides general conditions under which the conclusions of Theorem 2 also hold.

Proposition 7. *Suppose that there exist universal constants $C_k, C, c > 0$ such that $c < \max_{i,j} \text{Var}[Y_{i,j}^{(n)}] \leq C \min_{i,j} \text{Var}[Y_{i,j}^{(n)}]$ and $\mathbb{E}[\mathcal{E}_{i,j}^{(n)}]^{2k} \leq C_k (\text{Var}[Y_{i,j}^{(n)}])^k$ for all $i \in [m], j \in [n], n \geq 1$, and $k \geq 1$. Then, the conclusions of Theorem 2 hold for $\tilde{\Sigma}^{(n)} = n^{-1} \tilde{\mathcal{E}}^{(n)} (\tilde{\mathcal{E}}^{(n)})^T$, where $\tilde{\mathcal{E}}_{i,j}^{(n)} = u_i^{(n)} \mathcal{E}_{i,j}^{(n)} v_j^{(n)}$ and $(\mathbf{u}^{(n)}, \mathbf{v}^{(n)})$ is a solution to (16).*

The proof of Proposition 7 is obtained by repeating the proof outline of Theorem 2 and is omitted for the sake of brevity. Note that the proof of Theorem 3 does not directly rely on the particular distribution of $Y_{i,j}$ but only on the results of Theorem 2 and Equation (8). Hence, the conclusions of Theorem 3 would also hold for distributions of $Y_{i,j}$ satisfying the conditions in Proposition 7.

Continuing analogously to (13), we propose to estimate the scaling factors \mathbf{u} and \mathbf{v} by replacing the true variances $\{\text{Var}[Y_{i,j}]\}$ in (16) with corresponding independent unbiased estimators. That is, we propose to find positive $\hat{\mathbf{u}}$ and $\hat{\mathbf{v}}$ that satisfy

$$1 = \frac{1}{m} \sum_{i=1}^m \hat{u}_i^2 \widehat{\text{Var}}[Y_{i,j}] \hat{v}_j^2, \quad \text{and} \quad 1 = \frac{1}{n} \sum_{j=1}^n \hat{u}_i^2 \widehat{\text{Var}}[Y_{i,j}] \hat{v}_j^2, \quad (17)$$

where $\{\widehat{\text{Var}}[Y_{i,j}]\}_{i \in [m], j \in [n]}$ are independent, nonnegative, and satisfy $\mathbb{E}[\widehat{\text{Var}}[Y_{i,j}]] = \text{Var}[Y_{i,j}]$ for all $i \in [m]$ and $j \in [n]$. Lemma 4 and Theorem 5 can then be extended to distributions other than the Poisson by following our proof techniques and utilizing distribution-specific tail bounds.

Overall, Algorithm 1 can be adapted to a distribution other than the Poisson by replacing Y in Step 1 with the matrix of noise variance estimators $(\widehat{\text{Var}}[Y_{i,j}])_{i \in [m], j \in [n]}$, noting that existence and uniqueness of solutions to the scaling problem (17) depend on the zero pattern of this matrix as described at the end of Section 2.2 and in Appendix A.

4.1 Quadratic Variance Functions (QVFs)

We now consider a useful setting where $\widehat{\text{Var}}[Y_{i,j}]$ can be computed directly from $Y_{i,j}$. Suppose that the entries of Y belong to a family of distributions that satisfies a quadratic relation between the mean and the variance, namely

$$\text{Var}[Y_{i,j}] = a + bX_{i,j} + cX_{i,j}^2, \quad (18)$$

for all $i \in [m], j \in [n]$, where a, b, c are fixed constants. Evidently, the Poisson model (5) satisfies (18) with $a = c = 0$ and $b = 1$. To clarify the nomenclature, the term ‘family of distributions’ in the context of the Poisson refers to the set of Poisson distributions with all possible Poisson parameters.

Perhaps the most studied families that satisfy the quadratic relation (18) are the Natural Exponential Families with Quadratic Variance Functions (NEF-QVFs) [57, 58]. The NEF-QVFs include six fundamental families: the normal with fixed variance ($b = c = 0, a > 0$), the Poisson ($a = c = 0, b = 1$), the binomial with fixed number of trials ($a = 0, b = 1, c < 0$), the negative binomial with fixed number of failures ($a = 0, b = 1, c > 0$), the gamma with fixed shape parameter ($a = b = 0, c > 0$), and a family known as the Generalized Hyperbolic Secant ($a > 0, b = 0, c > 0$). It was shown in [57] that these six fundamental families, together with all of their possible linear transformations (scaling and translation), convolutions (sum of k i.i.d variables), and divisions (the inverse of a convolution), form all possible NEF-QVFs. If the entries of Y belong one of these families, then $Y_{i,j}$ satisfies (18) with a distinct set of coefficients a, b, c (unique to a specific NEF-QVF family). The NEF-QVFs also admit many favorable properties and satisfy the moment condition required in Proposition 7 (see Theorem 3 in [57] and the discussion immediately following the proof).

We now have the following proposition.

Proposition 8 (Unbiased variance estimator for QVFs). *If the entries of Y satisfy the QVF (18) with $c \neq -1$, then an unbiased variance estimator for $Y_{i,j}$ is given by*

$$\widehat{\text{Var}}[Y_{i,j}] = \frac{a + bY_{i,j} + cY_{i,j}^2}{1 + c}. \quad (19)$$

Among all of NEF-QVFs, the family of distributions consisting of the Bernoulli and its linear transformations is the only one with $c = -1$. For this family there is no unbiased variance estimator that is only a function of $Y_{i,j}$.

The proof can be found in Appendix K. Proposition 8 shows that all NEF-QVFs except the Bernoulli (and its linear transformations) admit unbiased variance estimators that can be easily computed from $Y_{i,j}$. More generally, our methodology is applicable to any family of distributions satisfying a generic QVF (18) (with $c \neq -1$), not just NEF-QVFs. Such families include the Generalized Poisson [18] with fixed dispersion, the log-normal with fixed variance (of the natural logarithm), the beta with fixed sample size (the sum of the two shape parameters), and the beta-binomial with fixed number of trials and intra-class correlation parameters, among (infinitely-many) other families of distributions. We note that since the quadratic variance relation (18) involves only the first and second moments, the higher moments of a distribution with a QVF can be arbitrary. Hence, the coefficients a, b, c do not uniquely identify a specific family of distributions in general.

In Appendix D we conduct numerical experiments analogous to the ones in Section 3.1 on three families of distributions: the binomial, negative binomial, and generalized Poisson. For these families we demonstrate the convergence of the spectrum of the noise after scaling to the MP law empirically (using the variance estimator (19) as well as the true variance (18)).

4.2 Missing entries and zero-inflation

It is worthwhile to mention that the QVF (18) can also accommodate for entries missing at random when imputed with zeros, or equivalently, if some of the entries are randomly assigned a zero value (i.e., zero inflation). In particular, suppose that we observe

$$\bar{Y}_{i,j} = \begin{cases} Y_{i,j}, & \text{with probability } p, \\ 0 & \text{with probability } 1 - p, \end{cases} \quad (20)$$

for some $p \in (0, 1]$, where the entries of Y satisfy the QVF (18). Then, we have $\bar{X} := \mathbb{E}[\bar{Y}] = pX$, whose rank is the same as X , and a direct calculation shows that

$$\text{Var}[\bar{Y}_{i,j}] = ap + bpX_{i,j} + p(c + 1 - p)X_{i,j}^2 = ap + b\bar{X}_{i,j} + \left(\frac{c + 1 - p}{p}\right)\bar{X}_{i,j}^2. \quad (21)$$

Consequently, the observation model (20) satisfies a QVF of the form (18) with coefficients that depend on the observation probability p . Then, the corresponding variance estimator is

$$\widehat{\text{Var}}[\bar{Y}_{i,j}] = \frac{ap^2 + bp\bar{Y}_{i,j} + (1+c-p)\bar{Y}_{i,j}^2}{1+c}. \quad (22)$$

Note that the variance estimator ends up with a quadratic term $\bar{Y}_{i,j}^2$ even if the QVF of $Y_{i,j}$ has $c = 0$. Therefore, our biwhitening approach can be useful even in a setting of homoskedastic noise ($a > 0$, $b = c = 0$) with missing entries, in which case the noise becomes heteroskedastic and satisfies a nontrivial QVF.

5 Practical considerations and real data

5.1 Adapting to the data

When analyzing experimental data, it is desirable to have a practical approach for finding the most appropriate coefficients in the QVF (18) automatically. To that end, we focus on QVFs with $a = 0$, $b \geq 0$, and $c \geq 0$. Such QVFs are naturally found in certain families of nonnegative random variables. In particular, any family that includes distributions with nonnegative variables with zero means must satisfy $a = 0$ (since a nonnegative random variable with zero mean must have zero variance). The restriction $b \geq 0$ and $c \geq 0$ is convenient to insure that the variance estimator (19) is always nonnegative if $Y_{i,j}$ is nonnegative. Substituting $a = 0$, $b = \alpha(1 - \beta)/(1 - \alpha\beta)$, and $c = \alpha\beta/(1 - \alpha\beta)$ in (19) for any $\beta \in [0, 1]$ and $\alpha > 0$, gives

$$\widehat{\text{Var}}[Y_{i,j}] = \alpha [(1 - \beta)Y_{i,j} + \beta Y_{i,j}^2]. \quad (23)$$

Intuitively, the parameter $\beta \in [0, 1]$ interpolates between a purely linear variance function and a purely quadratic variance function, whereas $\alpha > 0$ controls the global scaling.

Let us fix $\alpha = 1$ and some $\beta \in [0, 1]$. For a given matrix Y , the scaling equations (17) can be solved when plugging the variance estimator (23), providing the pair of scaling factors $(\hat{\mathbf{u}}, \hat{\mathbf{v}})$. The scaled data matrix is then given by $\hat{Y} = D(\hat{\mathbf{u}})YD(\hat{\mathbf{v}})$, and the corresponding Gram matrix is defined as $\hat{\Sigma} = n^{-1}\hat{Y}\hat{Y}^T$. Importantly, since α controls the global scaling of the matrix $(\widehat{\text{Var}}[Y_{i,j}])_{i \in [m], j \in [n]}$, it is clear from the equations (17) that the pair of scaling factors that solves (17) for any $\alpha > 0$ is given by $(\alpha^{-1/4}\hat{\mathbf{u}}, \alpha^{-1/4}\hat{\mathbf{v}})$. Consequently, the scaled data matrix for any $\alpha > 0$ is given by $\alpha^{-1/2}\hat{Y}$, and the corresponding Gram matrix is $\alpha^{-1}\hat{\Sigma}$. Note that the eigenvalues of $\alpha^{-1}\hat{\Sigma}$ are related to those of $\hat{\Sigma}$ by the scalar multiple α^{-1} .

We now propose a method for choosing α and β automatically from Y by minimizing the discrepancy between the spectrum of the resulting scaled data matrix and the MP law (relying on the fact that a low-rank perturbation of the scaled noise matrix $\hat{\mathcal{E}}$ does not change its limiting spectral distribution). For any fixed $\beta \in [0, 1]$, we choose α by matching the median of the eigenvalues of $\alpha^{-1}\hat{\Sigma}$ to the median of the MP distribution $F_{\gamma,1}$. That is, we take

$$\alpha = \frac{\lambda_{\text{med}}\{\hat{\Sigma}\}}{\mu_\gamma}, \quad (24)$$

where $\gamma = m/n$, $\lambda_{\text{med}}\{\hat{\Sigma}\}$ is the median eigenvalue of $\hat{\Sigma}$ (which depends on the value of β), and μ_γ is the median of the MP distribution with parameter γ and noise variance 1, i.e., μ_γ is the unique solution to the equation

$$F_{\gamma,1}(t) = \int_{\beta_-}^t \frac{\sqrt{(\tau - \beta_-)(\beta_+ - \tau)}}{2\pi\gamma\tau} d\tau = \frac{1}{2}, \quad (25)$$

in the variable $t \in (\beta_-, \beta_+)$, and $\beta_\pm = (1 \pm \sqrt{\gamma})^2$. Our approach here for choosing α is equivalent to the method proposed in [25] for estimating σ in the MP density (3). The use of the median in this context is advantageous due its robustness to outlier eigenvalues, e.g., signal components or finite-sample fluctuations of the noise eigenvalues at the edges of the spectrum. Then, we choose $\beta \in [0, 1]$ that minimizes the Kolmogorov-Smirnov (KS) distance

$$\sup_x \left| F_{[\alpha^{-1}\hat{\Sigma}]}(x) - F_{\gamma,1}(x) \right|, \quad (26)$$

where $F_{\gamma,1}$ is the MP distribution, $F_{[\alpha^{-1}\hat{\Sigma}]}$ is the ESD of $\alpha^{-1}\hat{\Sigma}$ (see (2)), and we emphasize that $\hat{\Sigma}$ and α depend on the value of β . Since the minimization over all $\beta \in [0, 1]$ is intractable (as it involves

solving (17) for each β separately), we propose to approximate this minimization by scanning over a finite grid of values in $[0, 1]$.

We demonstrate the above approach numerically in Appendix E on a simulated negative binomial matrix. We consider both a situation where the number of negative binomial failures is fixed across the entries in the matrix, and also a situation where the number of negative binomial failures is varying – exemplifying the robustness of our approach to certain violations of the QVF model (18).

In order to validate a certain choice of α and β in our framework, it is natural to consider the quality of the fit of the spectrum after scaling to the MP law (assuming that the rank of the signal matrix is sufficiently small). To account for the bias in the selection procedure of α and β , we propose to make use of a sample splitting scheme as follows. First, we determine α and β from a submatrix of Y (e.g., half the columns of Y) as described in this section. Then, we treat α and β as known model parameters to solve (17) on a disjoint submatrix (e.g., the remaining columns), and measure the fit of the spectrum after scaling to the MP law. For the measure of goodness-of-fit, we use the Kolmogorov-Smirnov (KS) test (whose statistic is the quantity minimized in (26) to choose β for a disjoint submatrix). This procedure is repeated several times on randomly-chosen submatrices and the results (KS distances, p-values) are averaged across trials. We note that the null hypothesis underlying this methodology is that the eigenvalues of the scaled data matrix are sampled independently from the MP distribution. While this assumption does not strictly hold (due to the existence of signal components in the data, and also since the eigenvalues of a random noise matrix are dependent), it serves as a useful surrogate null hypothesis that allows for an interpretable measure of goodness-of-fit.

5.2 Fit to the MP law for real data

We now exemplify our biwhitening approach on several real datasets from three domains of application: Single-Cell RNA Sequencing (scRNA-seq), High-Throughput Chromosome Conformation Capture (Hi-C), and document topic modeling. For scRNA-seq, we used the well-studied purified Peripheral Blood Mononuclear Cells (PBMCs) dataset from Zheng et al. [75], and the dataset by Hrvatin et al. [38] that contains mouse visual cortex cells. For Hi-C, we used the dataset by Johanson et al. [41] from Naïve CD4+ T cells from homo-sapiens, where we extracted the submatrix of interactions between chromosomes one and two (the largest chromosomes), corresponding to 4622×4822 different pairs of loci. For document topic modeling, we used the Associated Press dataset [31] (containing 10473 terms in 2246 documents), and the 20 NewsGroups dataset [49] (containing 61188 terms in 18774 documents).

We applied downsampling and filtering steps to the datasets to control their size and sparsity; see Appendix C.4.1 for more details. Then, we applied the procedure described in Section 5.1 to find $\alpha > 0$ and $\beta \in \{0, 0.05, 0.1, \dots, 0.95, 1\}$ automatically from half the observations (half the cells in each scRNA-seq dataset, half the loci in chromosome 1 in the Hi-C dataset, and half the documents in each topic modeling dataset), and employed the resulting variance estimator (23) for the remaining half of the observations to find the scaling factors $(\hat{\mathbf{u}}, \hat{\mathbf{v}})$ and compute the scaled matrix $\hat{Y} = D(\hat{\mathbf{u}})YD(\hat{\mathbf{v}})$.

Figure 5 depicts the fit of the histogram of the eigenvalues of $n^{-1}\hat{Y}\hat{Y}^T$ to the MP law for each of the above-mentioned datasets (on the held-out part of the data matrix). For comparison, we also show the analogous fits for the standard Poisson variance estimator $\widehat{\text{Var}}[Y_{i,j}] = Y_{i,j}$, as well as for a constant variance estimator $\widehat{\text{Var}}[Y_{i,j}] = \alpha$, i.e., assuming homoskedastic noise with unknown variance, where α is set according to (24). To provide an interpretable measure of goodness-of-fit, we applied the KS test as described at the of Section 5.1 over 10 randomized trials. The averaged KS distances and the corresponding p-values are summarized in Table 1. The average chosen parameters were $\alpha = 1.02$, $\beta = 0$ for the Hi-C dataset, $\alpha = 1.01$, $\beta = 0.2$ for the PBMC dataset, $\alpha = 1.02$, $\beta = 0.41$ for the Hrvatin et al. dataset, $\alpha = 0.88$, $\beta = 1$ for the AP dataset, and $\alpha = 0.95$, $\beta = 1$ for the 20 NewsGroups dataset.

It is evident that for each of the five datasets, the spectrum of the original counts does not agree with the MP law even after adjusting for an unknown scalar noise variance. Indeed, the p-values from the KS test in this case are all extremely small. Hence, none of these datasets can be assumed to have homoskedastic noise. On the other hand, the simple Poisson model is already useful for the Hi-C data, as it provides an excellent fit to the MP law, which is improved only slightly after quadratic variance adjustment (selecting parameters that are very close to those of the standard Poisson). For all other datasets the Poisson model is inadequate, but we obtain accurate fits to the MP law using the quadratic variance estimator (23) with the chosen parameters α and β . In particular, the p-values after the quadratic variance adjustment are in a range where the KS test cannot be rejected with high significance (implying that it is quite likely to obtain the observed KS distance if the eigenvalues are actually sampled from the MP distribution). These results suggest that many real-world datasets can be scaled appropriately

Table 1: Goodness-of-fit between the eigenvalues of $n^{-1}\hat{Y}\hat{Y}^T$ and the MP law for several real datasets, where the scaling factors ($\hat{\mathbf{u}}, \hat{\mathbf{v}}$) were obtained by solving (17) for three different variance estimators: constant, Poisson, and the quadratic variance (23). The entries in the table were obtained by averaging the results from 10 randomized trials according to the sample splitting scheme described at the end of Section 5.1

Dataset	$\widehat{\text{Var}}[Y_{i,j}] = \alpha$		$\widehat{\text{Var}}[Y_{i,j}] = Y_{i,j}$		$\widehat{\text{Var}}[Y_{i,j}] = \alpha[(1 - \beta)Y_{i,j} + \beta Y_{i,j}^2]$	
	KS distance	p-value	KS distance	p-value	KS distance	p-value
PBMC	0.21	10^{-211}	0.03	10^{-6}	0.007	0.95
Hrvatin et al.	0.24	10^{-250}	0.17	10^{-131}	0.01	0.26
Hi-C	0.07	10^{-10}	0.01	0.85	0.005	0.99
AP	0.18	10^{-31}	0.14	10^{-20}	0.02	0.37
20 NewsGroups	0.2	10^{-103}	0.15	10^{-47}	0.02	0.1

(by diagonal scaling) to make the empirical spectral distribution very close to the MP law, allowing for adaptive signal detection. Interestingly, the chosen α and β for the scRNA-seq datasets agree well with a negative binomial model (where $b = 1$). The negative binomial is a standard model for scRNA-seq data, explained by a Poisson observation model with a gamma prior on the Poisson parameter [65].

5.3 Rank estimation on annotated data

To test the accuracy of our rank estimation method on real data, we used the class labels available for the cells in the PBMC dataset and the labels for the documents in the 20 NewsGroups dataset. We first randomly selected 500 observations from each one of several classes, and then filtered the resulting matrices for sparsity. For the PBMC dataset we used 8 classes out of 10, and for the 20 NewsGroups we used 10 classes out of 20, choosing classes that should be well distinguishable; see more details in Appendix C.4.2. Since the number of classes is generally not equal to the rank of the signal matrix but is only a lower bound (assuming that the classes correspond to subspaces that are linearly independent), we further performed the following ‘‘homogenization’’ procedure. We randomly permuted the entries in each feature (a gene in the PBMC dataset and a word in the 20 NewsGroups dataset) across all observations in a class, for each class and each feature independently. This homogenization destroys the correlations that exist across observations or features within a class, so the resulting underlying signal matrix has as many large eigenvalues as the number of classes and the rest of the eigenvalues should be very small. While this homogenization undoubtedly removes information from the data (the within-class structure), it allows us to use the number of classes as a surrogate for the rank while preserving important characteristics of the data, such as the distribution of values within each feature and each class.

Figure 6 illustrates the sorted singular values of the resulting homogenized matrices before and after biwhitening, where we used our adaptive version described in Section 5.1 to choose $\alpha > 0$ and $\beta \in \{0, 0.05, \dots, 1\}$ automatically. It is evident that the signal singular values are more easily detectable after biwhitening and emerge above the MP upper edge (noting that the 8th signal singular value for the PBMC dataset is slightly above the MP upper edge but too close to it to be clearly visible). We repeated our data preprocessing and homogenization procedure for 10 randomized trials, each time estimating the rank by applying our method as well as the other methods described in Section 3.2. Table 2 summarizes the average estimated ranks and their standard deviations. Overall, it is evident that our method provides the most accurate rank estimates for both datasets, while other methods consistently overselect or underselect the rank.

6 Discussion

Our biwhitening procedure for rank estimation has several important advantages over alternative methods. First and foremost, it can handle almost any pattern of entries in X , including those that lead to severe noise heteroskedasticity. In particular, and as suggested by our simulations in Section 3.2, our method stabilizes the noise variances across rows and columns and prevents extreme rows or columns from dominating the spectrum of the noise, allowing our method to detect weak signal components that

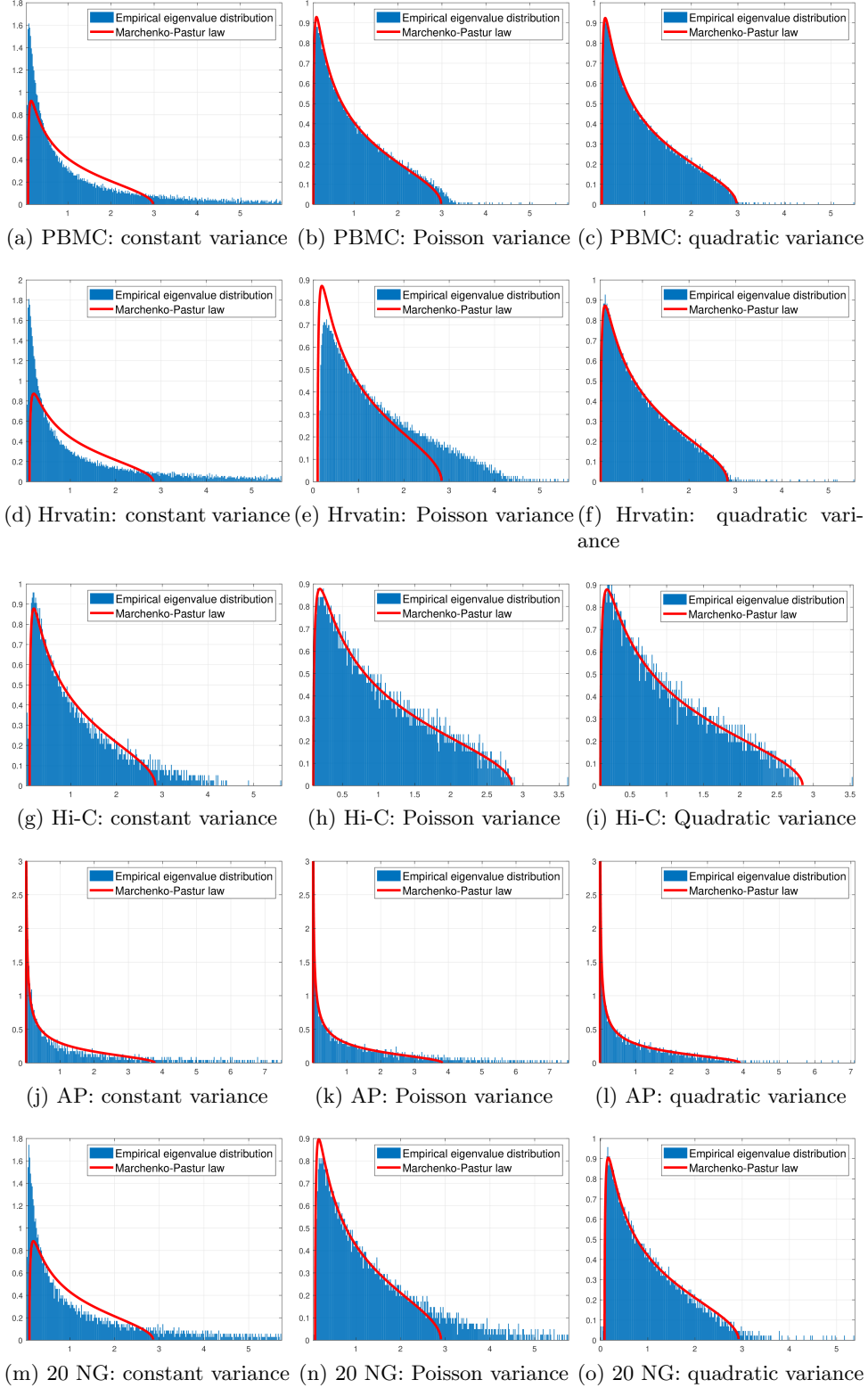
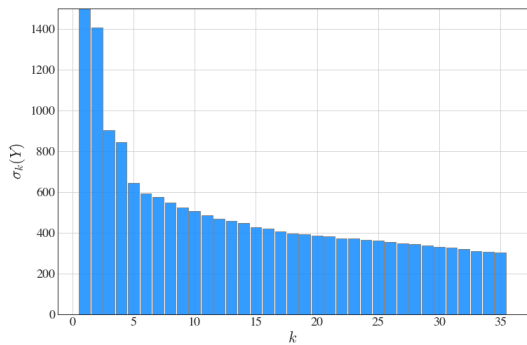
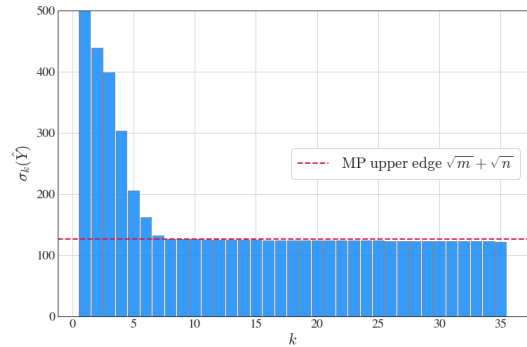


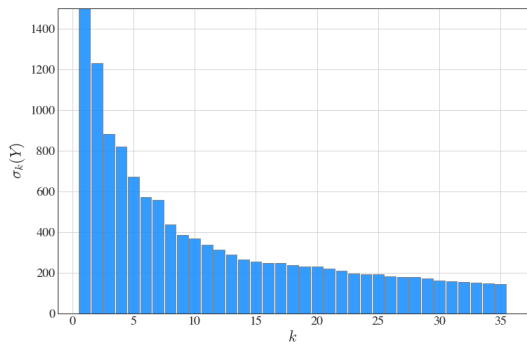
Figure 5: Eigenvalue histograms obtained from several datasets (from top to bottom): Purified PBMC [75], Hrvatin et al. [38], Hi-C [41], Associated Press [31], and 20 NewsGroups (20 NG) [49], versus the Marchenko-Pastur density $dF_{\gamma,1}$, where $\gamma = m/n$. For each dataset, we used three variance estimators (from left to right) when solving (17): constant variance ($\widehat{\text{Var}}[Y_{i,j}] = \alpha$, where α is chosen by (24)), Poisson variance ($\widehat{\text{Var}}[Y_{i,j}] = Y_{i,j}$), and adjusted quadratic variance (Eq. (23), where α and β are chosen as described in Section 5.1). The eigenvalue histograms are shown for a held-out subset of the data matrix (whereas α and β are determined from a disjoint subset of the data matrix).



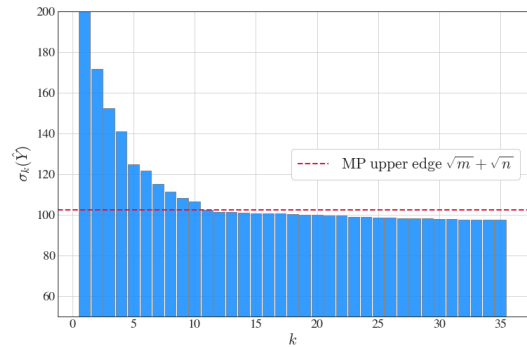
(a) Homogenized PBMC, original counts



(b) Homogenized PBMC, after biwhitening



(c) Homogenized 20 NewsGroups, original counts



(d) Homogenized 20 NewsGroups, after biwhitening

Figure 6: Sorted singular values of the homogenized matrices for the PBMC dataset (top) and the 20 NewsGroups dataset (bottom) before (left) and after (right) biwhitening. For the PBMC dataset we used 8 classes (cell types), and for the 20 NewsGroups we used 10 classes (news groups), hence the expected ranks are 8 and 10, respectively (see the details of homogenization). To perform biwhitening we used the procedure described in Section 5.1 to find $\alpha > 0$ and $\beta \in \{0, 0.05, \dots, 1\}$ adaptively.

Table 2: Mean (standard deviation) of ranks selected by several methods (see Section 3.2) for two real datasets with ground truth labels. The datasets were preprocessed and homogenized (observations with the same label were randomly permuted along each feature independently) over 10 randomized trials.

Dataset	r	Our method	EKC	pairPA	DDPA+	Signflip PA
PBMC	8	8.4 (0.7)	21.7 (3.1)	69.1 (1.9)	100.5 (68.6)	5 (0.0)
20 NewsGroups	10	10 (0.0)	40.2 (11.2)	9.6 (1.4)	3.1 (0.7)	14.2 (0.9)

otherwise would be masked by the noise. Second, our method enforces the largest noise eigenvalue to admit a simple analytic expression – the MP upper edge. This property obviates the need for estimating the largest noise eigenvalue by Monte Carlo simulations (such as permutations and signflips of the data), which are sensitive to the structure and magnitude of the unknown signal matrix. Lastly, our approach provides a simultaneous validation of our model assumptions through the fit of the resulting spectrum to the MP law. Such validation is an invaluable tool for exploratory data analysis, where ground truth information is seldom available.

Since this work is concerned with rank estimation, it is worthwhile to discuss the closely related task of recovering the principal components. In [33] it was shown that the performance of standard PCA can significantly degrade under heteroskedastic noise, even if the noise varies only along one dimension of the matrix. Therefore, while our approach is able to accurately detect informative signal components in heteroskedastic noise, it may be suboptimal to plug our estimated rank directly into standard PCA when the noise is strongly heteroskedastic. In such cases, one possibility is to apply our method in conjunction with recently proposed methods for PCA and matrix denoising under heteroskedastic noise; see e.g., [74] (or special cases such as Poisson noise [13]), which require knowledge of the rank. Another possibility is to apply standard PCA after biwhitening, which is particularly appealing since biwhitening stabilizes the average noise variances across rows and columns, alleviating much of the effect of heteroskedastic noise. However, the scaling of rows and columns introduces a bias into the principal components, modifying them in a nontrivial way. In certain applications this may be acceptable, and applying PCA after biwhitening can be favorable if more principal components are detected and utilized for subsequent analysis. In other applications, where interpretability of the principal components is important, the bias introduced by the scaling may need to be corrected. This topic is a promising future research direction but is beyond the scope of this paper and is left for future work.

7 Acknowledgements

The authors would like to thank Edgar Dobriban, George Linderman, Jay Stanley, and Xiaou Li for useful and insightful discussions. B.L., T.Z., and Y.K. acknowledge support by NIH grant R01GM131642. B.L. and Y.K. also acknowledge support by NIH grants UM1DA051410, U01DA053628, and U54AG076043. Y.K. acknowledges support by NIH grants R01GM135928 and 2P50CA1219.

Appendix A Existence and uniqueness of \mathbf{x} and \mathbf{y} in (11) for $r_i = n$ and $c_j = m$

We begin with the following definition.

Definition 9 (Completely decomposable matrix). We say that a nonnegative matrix $A \in \mathbb{R}^{m \times n}$ is *completely decomposable* if there exist proper nonempty subsets $\mathcal{I}_1 \subset [m]$ and $\mathcal{I}_2 \subset [n]$ such that $[A]_{i \in \mathcal{I}_1, j \in \mathcal{I}_2}$ and $[A]_{i \in \mathcal{I}_1^c, j \in \mathcal{I}_2^c}$ are both zero matrices, where $[A]_{i \in \mathcal{I}_1, j \in \mathcal{I}_2}$ is the submatrix of A obtained by taking its rows in \mathcal{I}_1 and columns in \mathcal{I}_2 , and \mathcal{I}_1^c and \mathcal{I}_2^c are the complements of \mathcal{I}_1 and \mathcal{I}_2 in $[m]$ and $[n]$, respectively. In other words, A is completely decomposable if there exist permutation matrices $P \in \mathbb{R}^{m \times m}$ and $Q \in \mathbb{R}^{n \times n}$ such that

$$PAQ = \begin{bmatrix} B_{1,1} & \mathbf{0}_{|\mathcal{I}_1| \times |\mathcal{I}_2|} \\ \mathbf{0}_{|\mathcal{I}_1^c| \times |\mathcal{I}_2^c|} & B_{2,2} \end{bmatrix}, \quad (27)$$

where $\mathbf{0}_{d_1 \times d_2}$ is a matrix of zeros of size $d_1 \times d_2$. We say that A is *not completely decomposable* if P and Q such as in (27) do not exist.

A useful equivalent characterization of a completely decomposable matrix can be obtained by inspecting the connectivity of the bipartite graph described by A . Specifically, consider the undirected and unweighted bipartite graph $\mathcal{G}_A(\mathcal{U}, \mathcal{V}, E)$ whose nodes \mathcal{U} correspond to the rows of A , nodes \mathcal{V} correspond to the columns of A , and edges E between \mathcal{U} and \mathcal{V} correspond to the nonzero entries of A , i.e., the i 'th node in \mathcal{U} is connected to the j 'th node in \mathcal{V} if and only if $A_{i,j} > 0$. Then, it immediately follows that A is completely decomposable if and only if the graph \mathcal{G}_A is disconnected, and furthermore, the connected components of \mathcal{G}_A correspond to the blocks $B_{1,1}$ and $B_{2,2}$ in (27) after permuting the nodes \mathcal{U} and \mathcal{V} according to P and Q from (27), respectively.

We now consider two important zero patterns of A . First, it is clear that if A admits any zero row or column, then \mathbf{x} and \mathbf{y} that solve (11) cannot exist. Hence, any zero rows or columns in a realization of

Y must first be removed before attempting to solve (13). Second, observe that according to (27), if A is completely decomposable and does not have any zero rows or columns, then after a certain permutation of its rows and columns it can be written as a direct sum of smaller nonnegative matrices that are not completely decomposable. In other words, if each row and column of A has at least one positive entry, then there exist permutation matrices P and Q such that

$$PAQ = \bigoplus_{k=1}^K B_{k,k} = \begin{bmatrix} B_{1,1} & \mathbf{0} & \mathbf{0} & \mathbf{0} \\ \mathbf{0} & B_{2,2} & \mathbf{0} & \mathbf{0} \\ \mathbf{0} & \mathbf{0} & \ddots & \mathbf{0} \\ \mathbf{0} & \mathbf{0} & \mathbf{0} & B_{K,K} \end{bmatrix}, \quad (28)$$

where \bigoplus is the direct sum operation, $B_{k,k} \in \mathbb{R}^{d_1^{(k)} \times d_2^{(k)}}$ are nonnegative matrices that are not completely decomposable, and $\mathbf{0}$ represents a block of zeros of appropriate size (not necessarily square). Importantly, since permuting rows and columns does not change their sums, the task of scaling A to row sums n and column sums m is equivalent to that of scaling each of the matrices $B_{k,k}$ to these row and column sums. However, scaling the matrix $B_{k,k} \in \mathbb{R}^{d_1^{(k)} \times d_2^{(k)}}$ to row sums n and column sums m is possible only if

$$d_1^{(k)} n = d_2^{(k)} m, \quad (29)$$

since the sum of all row sums is equal to the sum of all the entries in the matrix and must be the same as the sum of all column sums. Equation (29) implies that the aspect ratios (i.e., the number of columns divided by the number of rows) of each of the blocks $\{B_{k,k}\}$ must be exactly the same as the aspect ratio of matrix A , which is clearly a restrictive requirement.

To circumvent the above-mentioned issue, observe that whenever the realization of Y is completely decomposable, the singular value decomposition of Y can be written explicitly using the singular value decompositions of the blocks $\{B_{k,k}\}$ from the decomposition (28) of Y (replacing A). In particular, the singular values of Y are given by concatenating the singular values of each of the blocks $B_{k,k}$. This suggests that one should treat each block $B_{k,k}$ separately as a $d_1^k \times d_2^k$ matrix, and scale it accordingly to row sums d_2^k and column sums d_1^k . Correspondingly, the theory in Section 2 would apply to each block $B_{k,k}$ separately. Therefore, for a given realization of Y , we propose to first remove its zero rows and columns, and to find its blocks $B_{k,k}$ in the decomposition (28) by finding the connected components in the bipartite graph represented by Y . We then treat each block $B_{k,k}$ as a $d_1^k \times d_2^k$ matrix that should be scaled to row sums d_2^k and column sums d_1^k (instead of n and m , respectively), and the rank for each block $B_{k,k}$ should be chosen separately according to Section 2. Note that each $B_{k,k}$ does not have any zero rows and columns and is not completely decomposable, hence in what follows we proceed by treating the case where A assumes the same properties.

For a matrix A that does not have any zero rows and columns and is not completely decomposable, the following is the precise requirement from A so that positive \mathbf{x} and \mathbf{y} that satisfy (11) for $r_i = n$ and $c_j = m$ exist and are unique.

Condition 10. For all non-empty subsets $\mathcal{I}_1 \subset [m]$ and $\mathcal{I}_2 \subset [n]$ for which $[A]_{i \in \mathcal{I}_1, j \in \mathcal{I}_2}$ is a matrix of zeros, $|\mathcal{I}_1|n + |\mathcal{I}_2|m < mn$.

We then have the following proposition, which characterizes the existence and uniqueness of positive \mathbf{x} and \mathbf{y} that satisfy (11) for the case of $r_i = n$ and $c_j = m$.

Proposition 11 (Existence and uniqueness of \mathbf{x} and \mathbf{y} for $r_i = n$, $c_j = m$). *Let $r_i = n$ and $c_j = m$ for all $i \in [m]$ and $j \in [n]$ in (11), and suppose that A does not have any zero rows and columns and is not completely decomposable. Then, there exists a pair (\mathbf{x}, \mathbf{y}) of positive vectors that satisfies (11) if and only if Condition 10 holds. If such a pair (\mathbf{x}, \mathbf{y}) exists, it is unique up to a positive scalar, namely it can only be replaced with $(a\mathbf{x}, a^{-1}\mathbf{y})$ for any $a > 0$.*

Proof. Proposition 11 follows directly from Theorem 1 in [10]. Specifically, our Condition 10 is a equivalent to condition (1) in [10] for the case of $r_i = n$, $c_j = m$, and under the assumption that A is not completely decomposable. \square

Note that Condition 10 does not hold if A includes any zero submatrix whose number of rows and columns exceed $\lfloor m/2 \rfloor$ and $\lfloor n/2 \rfloor$, respectively. In more generality, we anticipate that positive \mathbf{x} and \mathbf{y} that satisfy (11) for the case of $r_i = n$ and $c_j = m$ might not exist if A is too sparse. Since Condition 10

as stated is somewhat obscure and is non-trivially verified from a given matrix A , it is worthwhile to provide a simpler condition only in terms of the number of zeros in the rows and columns of A . This is the purpose of the following proposition, which describes a sufficient condition for a matrix A to simultaneously satisfy Condition 10 and not be completely decomposable.

Proposition 12. *Suppose that A has no zero rows or columns and both requirements below are met:*

1. *For each $k \leq \lfloor n/2 \rfloor$, A has less than $\lceil mk/n \rceil$ rows that have at least $n - k$ zeros each.*
2. *For each $\ell \leq \lfloor m/2 \rfloor$, A has less than $\lceil n\ell/m \rceil$ columns that have at least $m - \ell$ zeros each.*

Then, Condition 10 holds and A is not completely decomposable.

The proof of Proposition 12 can be found in Appendix J.

Importantly, the conditions in Proposition 12 can be easily verified for any given matrix A by counting the number zeros in each row and each column. In case that a given matrix A does not satisfy these conditions, it can be modified by removing its sparsest rows and columns until these conditions are met. In particular, one can check if the rows (columns) of A are in violation of the requirements in Proposition 12, and if so remove the sparsest row (column) of A , repeating the process until no violations are found.

Appendix B Fit against the MP law for Poisson noise with $\gamma = 1/3, 1/4$

In Figure (7) we depict the results of the experiment described in Section 3.1 for the aspect ratios $\gamma = m/n = 1/3, 1/4$.

Appendix C Reproducibility details

C.1 Figure 1

We first generated an $m \times r$ matrix B by sampling its entries independently from the log-normal distribution with mean 0 and variance 4 (i.e., from $\exp(2Z)$, where $Z \sim \mathcal{N}(0, 1)$). Then, we generated an $r \times n$ matrix C by sampling its entries independently from the uniform distribution over $[0, 1]$. Lastly, we computed $X = BC$, normalized X by a scalar so that its average entry is 1, and sampled the entries of Y from the Poisson distribution as in (5). After generating Y , Algorithm 1 was applied to Y with scaling tolerance $\delta = 10^{-12}$.

C.2 Figures 2 and 3

We generated the matrix X by sampling its entries independently from $\text{Unif}(1, 2)$, namely, the uniform distribution over $[1, 2]$, and multiplied the resulting matrix from left and right by diagonal matrices whose entries (on the main diagonal) were sampled independently from $\exp(\text{Unif}(-2, 2))$. Then, each entry $Y_{i,j}$ was sampled independently from $\text{Poisson}(X_{i,j})$. Note that Theorems 2 and 5 in Section 2 do not make any assumptions about the rank of X , and indeed, in this experiment the matrix X has full rank with probability 1. After generating Y , we obtained the eigenvalues of the matrices $\Sigma_n = n^{-1}\mathcal{E}\mathcal{E}^\top$, $\hat{\Sigma}_n = n^{-1}\hat{\mathcal{E}}\hat{\mathcal{E}}^\top$, $\tilde{\Sigma}_n = n^{-1}\tilde{\mathcal{E}}\tilde{\mathcal{E}}^\top$ (corresponding to the original noise matrix, the biwhitened noise matrix using the estimated scalings factors, and the biwhitened noise matrix using the exact scaling factors, respectively). To compute these matrices, the Sinkhorn-Knopp algorithm (Algorithm 2) was used with tolerance $\delta = 10^{-11}$.

C.3 Rank estimation accuracy (Section 3.2)

For the first two experiments (Figures 4a and 4b), the Poisson parameter matrix was generated as $X = cUV$, $U \in \mathbb{R}^{500 \times 20}$, $V \in \mathbb{R}^{20 \times 750}$, where c is a positive scalar. For Figure 4a, we used $U_{ij} \sim \exp(\text{Unif}(-1, 1))$ and $V_{ij} \sim \text{Unif}(0, 1)$, whereas for Figure 4b we used $U_{ij} \sim \exp(2 \cdot \mathcal{N}(0, 1))$ and $V_{ij} \sim \text{Unif}(0, 1)$. In both cases we used the scalar c to control the average value of X . For the third experiment (Figure 4c), the Poisson parameter matrix was generated as $X = cUV + pq^\top$, $U \in \mathbb{R}^{500 \times 19}$, $V \in \mathbb{R}^{19 \times 750}$, and c is a positive scalar, where $U_{ij} \sim \exp(\text{Unif}(-1, 1))$, $V_{ij} \sim \text{Unif}(0, 1)$, and the rank-1 factor pq^\top was generated by sampling $p_i, q_j \in \exp(2 \cdot \mathcal{N}(0, 1))$. We then varied the scalar c to control the average value of the matrix cUV .

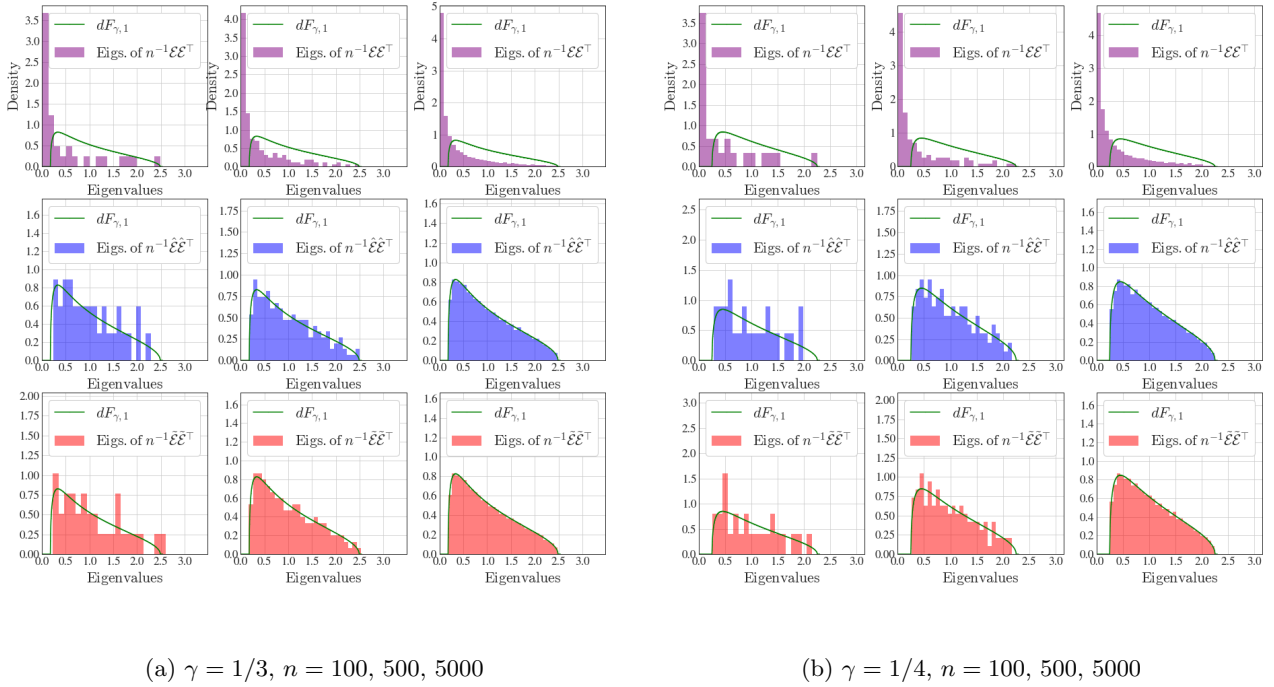


Figure 7: Spectrum of simulated Poisson noise versus the standard ($\sigma = 1$) Marchenko-Pastur density $dF_{\gamma,1}$, for aspect ratios $\gamma = m/n = 1/3, 1/4$ and matrix dimensions $n = 100, 500, 5000$ (from left to right in each panel). The top row in each panel (purple) corresponds to the eigenvalues of Σ_n (i.e., without any row or column scaling). The center row in each panel (blue) corresponds to the eigenvalues of $\hat{\Sigma}_n$ (i.e., after scaling with the estimated scaling factors). The bottom row in each panel (red) correspond to the eigenvalues of $\tilde{\Sigma}_n$ (i.e., after scaling with the exact scaling factors).

C.4 Experiments on real data

C.4.1 Fits to the MP law (Section 5.2)

For the PBMC dataset, for each trial of sample-splitting we randomly chose 20000 cells and split them into two equal groups to create two matrices. Then, for each of these matrices we removed all columns (genes) that had less than or equal to 200 nonzeros, and removed all rows (cells) that had less than or equal to 200 nonzeros in the resulting matrix. We applied the same pipeline to the Hrvatin dataset except that we initially retained 10000 cells from the data, and later used 100 as a threshold for the sparsity of genes and cells. For the Hi-C dataset, for each trial of sample-splitting we randomly split the loci of chromosome 1 into two equal groups to create two matrices. We then removed from each of them all columns (chromosome 1 loci) that had less than or equal to 10 nonzeros, and further removed all rows (chromosome 2 loci) that had less than or equal to 10 nonzeros in the resulting matrix. For the AP dataset, for each trial of sample-splitting we randomly split the documents into two groups to create two matrices. Then, we removed from each of them all columns (terms/words) with 30 or less nonzeros, and further removed all rows (documents) with 2 or less nonzeros in the resulting matrix. In addition, we removed duplicate documents and terms from the filtered matrices. For the 20 NewsGroups dataset, we used the same pipeline except that that we first randomly chose 10000 documents and removed 1% of the most popular terms across the chosen documents, before the rest of the sample splitting procedure and sparsity filtering.

C.4.2 Rank estimation with ground truth (Section 5.3)

For the PBMC dataset, each cell in the dataset was initially labelled with one of 10 cell types. We chose the following 8 cell types that should be well separated: ‘naive_t’, ‘b_cells’, ‘cd14_monocytes’, ‘naive_cytotoxic’, ‘memory_t’, ‘regulatory_t’, ‘cd56_nk’, and ‘cytotoxic_t’. We randomly sampled 500 cells from each type to form a matrix with 4000 columns, and removed the rows (genes) that have 100 or fewer nonzeros. For the 20 Newsgroups dataset, each document was initially labelled with one of 20 topics. We selected the following 10 topics: ‘alt.atheism’, ‘comp.sys.mac.hardware’, ‘comp.windows.x’, ‘misc.forsale’, ‘rec.motorcycles’, ‘rec.sport.hockey’, ‘sci.space’, ‘soc.religion.christian’, ‘talk.politics.guns’, ‘talk.politics.misc’. We then randomly chose 500 documents from each topic to form a matrix with 5000 columns. We removed the rows (terms) that had 100 or less nonzeros, and further removed the resulting zero columns.

Appendix D Fit against the MP law for several families with quadratic variance functions

In this section we provide results analogous to the ones described in Section 3.1 (fit of the spectrum of Poisson noise after scaling to the MP law) for the binomial, negative binomial, and generalized Poisson; see Section 4.1.

D.1 Binomial

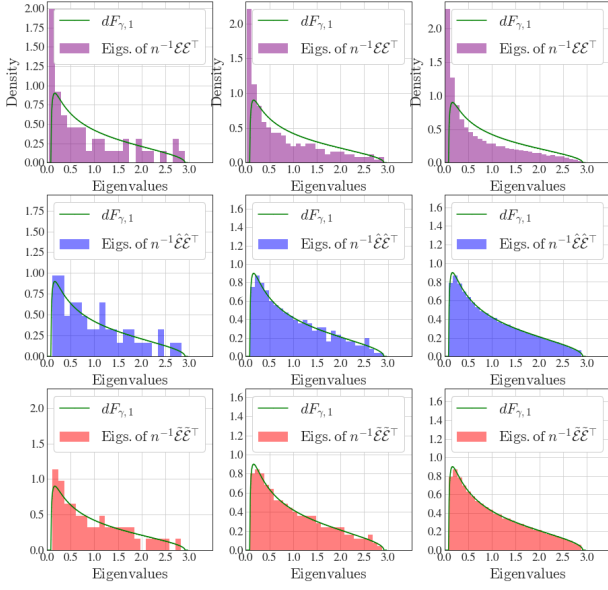
The binomial distribution depends on two parameters: the success probability and the number of trials. We generated the success probability matrix $P = (p_{i,j})_{i \in [m], j \in [n]}$ in the same way as we generated the Poisson parameter matrix X in Section 3.1 (see Appendix C.2), except that we also normalized each column to sum to 1. As for the number of binomial trials, we set it as a constant $\ell = 5$ for all $i \in [m]$, $j \in [n]$. Then, we sampled $Y_{i,j}$ independently from $\text{Binomial}(p_{i,j}, \ell)$. We used the true variances (18) with $a = 0$, $b = 1$, $c = -1/\ell$ and their unbiased estimators (19) to solve the systems of equations (16) and (17), respectively, using the Sinkhorn-Knopp algorithm with tolerance $\delta = 10^{-11}$. In Figure 8 we plot the eigenvalue histograms (normalized appropriately) of Σ_n , $\hat{\Sigma}_n$, and $\tilde{\Sigma}_n$, for aspect ratios $\gamma = m/n = 1/2, 1/3, 1/4, 1/5$ and column dimensions $n = 100, 500, 5000$. Similarly to the Poisson (Figure 2), we obtain an accurate fit to the MP law even for moderate matrix dimensions.

D.2 Negative Binomial

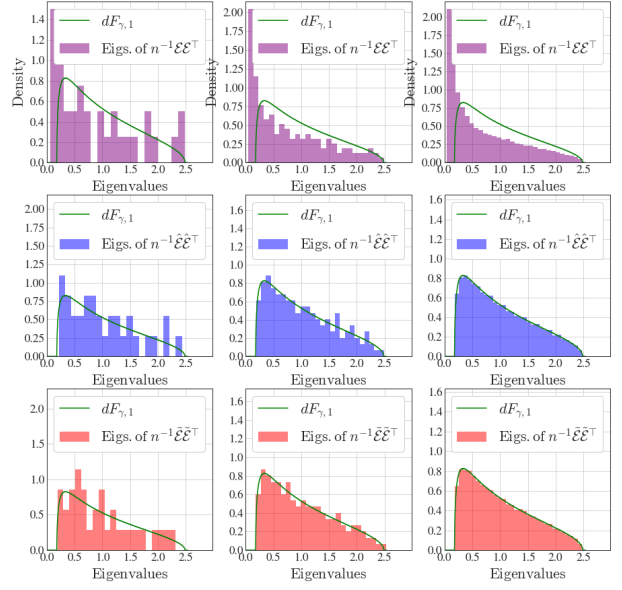
The negative binomial distribution depends on two parameters: the number of failures and the probability of success. In this experiment, we set the number of failures for all entries in the matrix to be $\rho = 3$. We generated the matrix X as for the experiment in Section 3.1 (see Appendix C.2), and formed the matrix of success probabilities for the negative binomials as $p_{i,j} = X_{i,j}/(r + X_{i,j})$. We then sampled each $Y_{i,j}$ independently from $\text{NegBinomial}(p_{i,j}, \rho)$, and computed the eigenvalues of Σ_n , $\hat{\Sigma}_n$, and $\tilde{\Sigma}_n$, where we used the true variance (18) with $a = 0$, $b = 1$, $c = 1/\rho$ and its unbiased estimator (23) to solve the systems of equations (16) and (17) (using the Sinkhorn-Knopp algorithm with tolerance $\delta = 10^{-11}$). In Figure 9 we plot the resulting eigenvalue histograms (normalized appropriately) of Σ_n , $\hat{\Sigma}_n$, and $\tilde{\Sigma}_n$, for aspect ratios $\gamma = m/n = 1/2, 1/3, 1/4, 1/5$ and column dimensions $n = 100, 500, 5000$. As before, the results are very similar to the ones in the Poisson case (Figure 2), demonstrating the convergence to the MP law as the dimensions grow.

D.3 Generalized Poisson

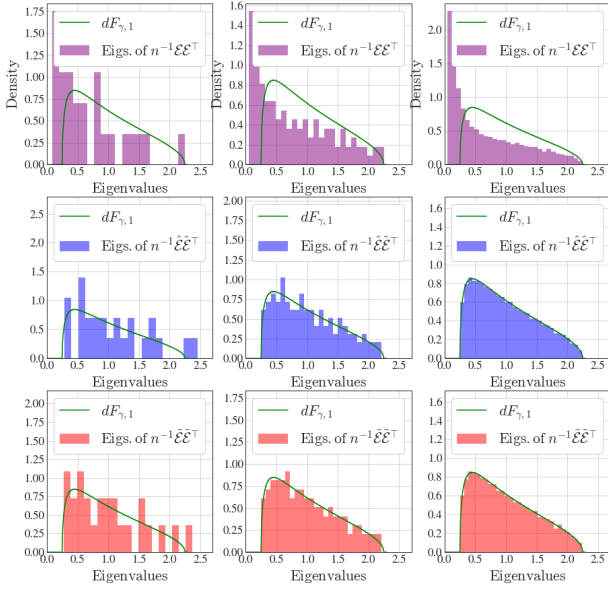
We simulated data from the Generalized Poisson distribution [18] as $Y_{i,j} \sim \text{GP}(X_{i,j}, \eta)$, where $X_{i,j}$ is the rate parameter and η is the dispersion parameter. We randomly generated the rate parameters $X_{i,j}$ in the same way as we generated the Poisson parameters in the example of Section 3.1 (see Appendix C.2), and fixed the dispersion parameter $\eta = 0.1$. We used the true noise variances (18) with $a = 0$, $b = 1/(1 - \eta)^2$, $c = 0$ (see [18]) and their unbiased estimators (19) to solve the systems of equations (16) and (17), respectively, using the Sinkhorn-Knopp algorithm with tolerance $\delta = 10^{-11}$. Next, we computed $\mathcal{E} = Y - \mathbb{E}[Y]$, $\Sigma_n = n^{-1}\mathcal{E}\mathcal{E}^T$, $\hat{\Sigma}_n = n^{-1}\hat{\mathcal{E}}\hat{\mathcal{E}}^T$, and $\tilde{\Sigma}_n = n^{-1}\tilde{\mathcal{E}}\tilde{\mathcal{E}}^T$. In Figure 10 we plot the eigenvalue histograms (normalized appropriately) of Σ_n , $\hat{\Sigma}_n$, and $\tilde{\Sigma}_n$, for aspect ratios $\gamma = m/n = 1/2, 1/3, 1/4, 1/5$



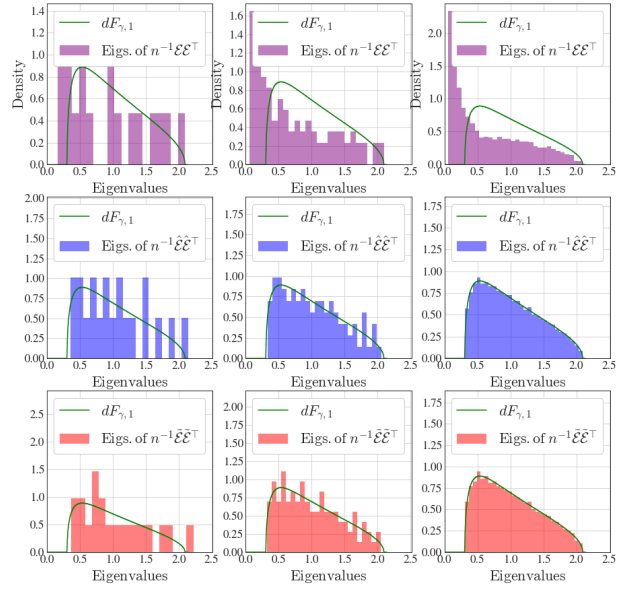
(a) $\gamma = 1/2$, $n = 100, 500, 5000$



(b) $\gamma = 1/3$, $n = 100, 500, 5000$

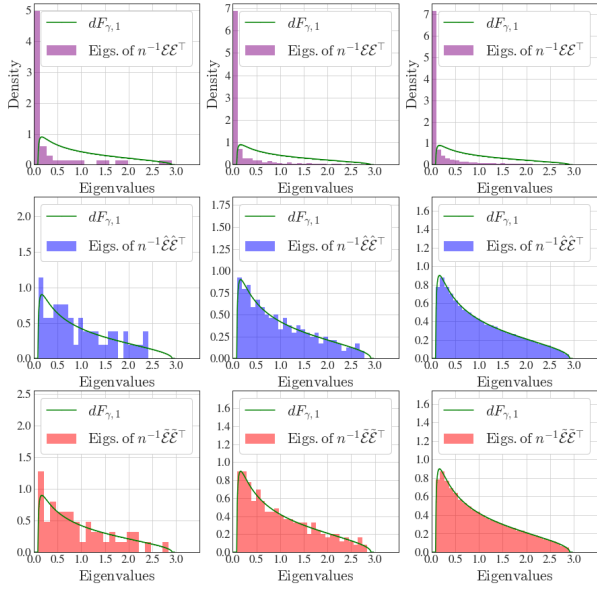


(c) $\gamma = 1/4$, $n = 100, 500, 5000$

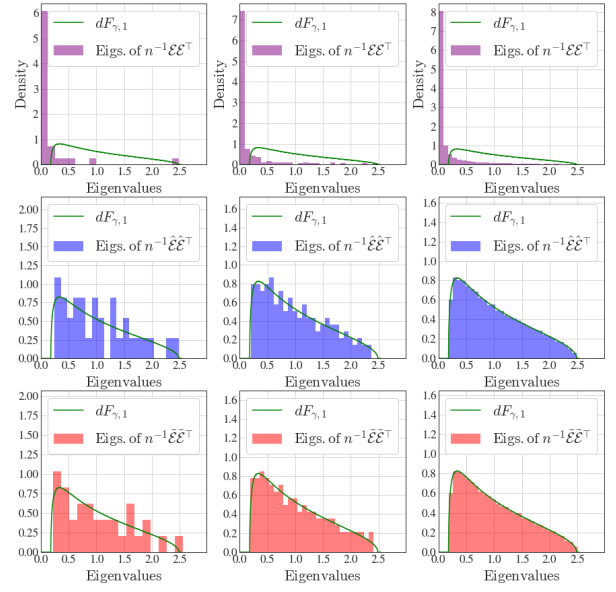


(d) $\gamma = 1/5$, $n = 100, 500, 5000$

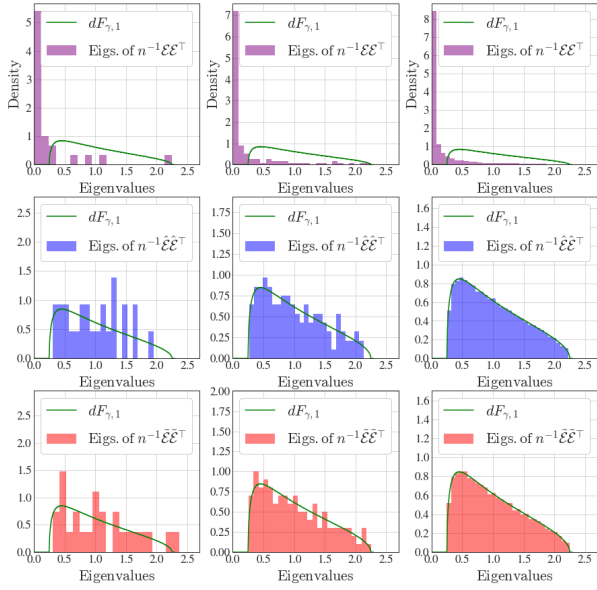
Figure 8: Spectrum of simulated binomial noise versus the standard ($\sigma = 1$) Marchenko-Pastur density $dF_{\gamma,1}$, for various aspect ratios γ and matrix dimensions $n = 100, 500, 5000$ (from left to right in each panel). The top row in each panel (purple) corresponds to the eigenvalues of Σ_n (i.e., without any row or column scaling). The center row in each panel (blue) corresponds to the eigenvalues of $\hat{\Sigma}_n$ (i.e., after scaling with the estimated scaling factors). The bottom row in each panel (red) correspond to the eigenvalues of $\tilde{\Sigma}_n$ (i.e., after scaling with the true scaling factors).



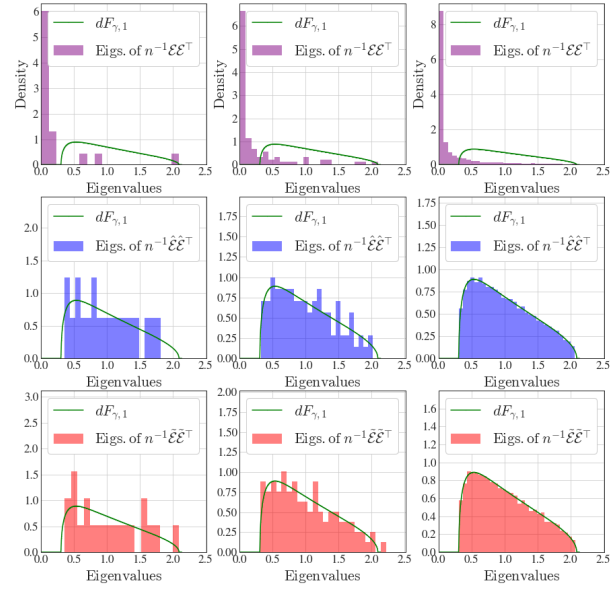
(a) $\gamma = 1/2$, $N = 100, 500, 5000$



(b) $\gamma = 1/3$, $N = 100, 500, 5000$



(c) $\gamma = 1/4$, $N = 100, 500, 5000$



(d) $\gamma = 1/5$, $N = 100, 500, 5000$

Figure 9: Spectrum of simulated negative binomial noise versus the standard ($\sigma = 1$) Marchenko-Pastur density $dF_{\gamma,1}$, for various aspect ratios γ and matrix dimensions $n = 100, 500, 5000$ (from left to right in each panel). The top row in each panel (purple) corresponds to the eigenvalues of Σ_n (i.e., without any row or column scaling). The center row in each panel (blue) corresponds to the eigenvalues of $\hat{\Sigma}_n$ (i.e., after scaling with the estimated scaling factors). The bottom row in each panel (red) correspond to the eigenvalues of $\tilde{\Sigma}_n$ (i.e., after scaling with the true scaling factors)

and column dimensions $n = 100, 500, 5000$. The results are very similar to the ones in the Poisson case (Figure 2), and we see an excellent fit to the MP law even for moderate matrix dimensions.

Appendix E Numerical experiments for Section 5.1

We exemplify the adaptive approach described in Section 5.1 on a simulated negative binomial matrix with $m = 1000$, $n = 2000$, and rank $r = 10$, where the number of negative binomial failures was set to 3. Consequently, the QVF satisfies $a = 0$, $b = 1$, $c = 1/3$, and it is easy to verify that the corresponding parameters in (23) are $\alpha = 1$ and $\beta = 0.25$. To create the matrix of negative binomial probabilities, we first generated $X = UV$, $U \in \mathbb{R}^{1000 \times 10}$, $V \in \mathbb{R}^{10 \times 2000}$, where $U_{i,j} \sim \exp(2 \cdot \mathcal{N}(0, 1))$ and $V_{i,j} \sim \exp(1 \cdot \mathcal{N}(0, 1))$. We then normalized X by a scalar to make its average entry equal to 1, and set the negative binomial failure probabilities as $p_{i,j} = X_{i,j}/(\rho_{i,j} + X_{i,j})$, where $\rho_{i,j}$ is the number of failures for $Y_{i,j} \sim \text{NegBinomial}(\rho_{i,j}, p_{i,j})$. This choice of $p_{i,j}$ ensures that $\mathbb{E}[Y_{i,j}] = X_{i,j}$.

Figure 11a depicts the KS distance (26) for the grid of values $\beta \in \{0, 0.05, \dots, 0.95, 1\}$. It is evident that the smallest KS distance is 0.01 and is attained for $\beta \in [0.2, 0.4]$ (each one with its corresponding α chosen according to (24)). The reason that the distance is saturated at 0.01 is that for these values of β the supremum in (26) is attained at $\tau = \beta_+$, where the distance is precisely $r/m = 0.01$. In order to compare between the estimated scaling factors $(\hat{\mathbf{u}}, \hat{\mathbf{v}})$ and the true scaling factors (\mathbf{u}, \mathbf{v}) , we eliminated the fundamental ambiguity in the scaling factors (see Proposition 1) by ensuring that $\|\mathbf{u}\|_1 = \|\mathbf{v}\|_1$ and $\|\hat{\mathbf{u}}\|_1 = \|\hat{\mathbf{v}}\|_1$. Figures (11b) and (11c) compare between the pair $(\hat{\mathbf{u}}, \hat{\mathbf{v}})$ and the pair (\mathbf{u}, \mathbf{v}) (each pair concatenated into a single vector) for the correct value $\beta = 0.25$ and for $\beta = 0.4$, which is the value furthest away from the correct β that achieves the minimal KS distance. As expected, the estimated scaling factors using $\beta = 0.25$ are nearly identical to the true scaling factors. However, the estimated scaling factors using $\beta = 0.4$ are also very close to the true scaling factors, and allow for an excellent fit to the MP law and correct rank estimation, as can be seen in Figure 12. We found empirically that all values of β that attain the smallest KS distance (which is $r/m = 0.01$) provide excellent fits to the MP law and lead to correct rank estimation.

In addition to the above, we conducted a similar experiment to demonstrate the robustness of the QVF assumption (18) to certain violations. Specifically, we randomly sampled the number of failures for each negative binomial entry uniformly at random from $\{1, \dots, 10\}$ (while keeping all other aspects of the experiment unchanged). Therefore, $\text{Var}[Y_{i,j}] = X_{i,j} + c_{i,j}X_{i,j}^2$, where $c_{i,j}$ is varying between 0.1 and 1 across different indices i, j , and no single QVF exists for Y . Nonetheless, according to the results in [48], the scaling factors of the matrix $(X_{i,j} + c_{i,j}X_{i,j}^2)_{i \leq m, j \leq n}$ are expected to concentrate around the scaling factors of the matrix $(X_{i,j} + \mathbb{E}[c_{i,j}]X_{i,j}^2)_{i \leq m, j \leq n}$, which corresponds to a standard QVF of the form (18) with $c = \mathbb{E}[c_{i,j}] = \sum_{k=1}^{10} k^{-1}/10 = 0.29$. Indeed, Figures 13 and 14 show that the procedure described in Section 5.1 can identify a range of parameters α and β that provide accurate estimates of the true scaling factors (\mathbf{u}, \mathbf{v}) (obtained from (16) using the true noise variances $\text{Var}[Y_{i,j}] = X_{i,j} + c_{i,j}X_{i,j}^2$), and consequently, an excellent fit to the MP law and correct rank estimation. Therefore, the assumption (18) can also serve as a useful approximation in situations where the parameters a, b, c are not constant but randomly perturbed (with respect to some baseline values).

Appendix F Proof of Theorem 2

Since the pair $(\mathbf{u}^{(n)}, \mathbf{v}^{(n)})$ is defined up to a constant, namely $(a\mathbf{u}^{(n)}, a^{-1}\mathbf{v}^{(n)})$ for any $a > 0$, we take a such that $\|\mathbf{u}^{(n)}\|_2 = \|\mathbf{v}^{(n)}\|_2$. Then, since $X^{(n)}$ is a positive matrix, applying Lemma 2 in [48] using $A = X^{(n)}$, $r_i = n$, $c_j = m$, $x_i = (u_i^{(n)})^2$ and $y_j = (v_j^{(n)})^2$, implies that

$$\begin{aligned} \sqrt{\frac{n \min_{i,j} X_{i,j}^{(n)}}{m_n (\max_{i,j} X_{i,j}^{(n)})^2}} \leq (u_i^{(n)})^2 \leq \sqrt{\frac{m_n \max_{i,j} X_{i,j}^{(n)}}{n (\min_{i,j} X_{i,j}^{(n)})^2}}, \\ \sqrt{\frac{n \min_{i,j} X_{i,j}^{(n)}}{m_n (\max_{i,j} X_{i,j}^{(n)})^2}} \leq (v_j^{(n)})^2 \leq \sqrt{\frac{m_n \max_{i,j} X_{i,j}^{(n)}}{n (\min_{i,j} X_{i,j}^{(n)})^2}}, \end{aligned} \tag{30}$$

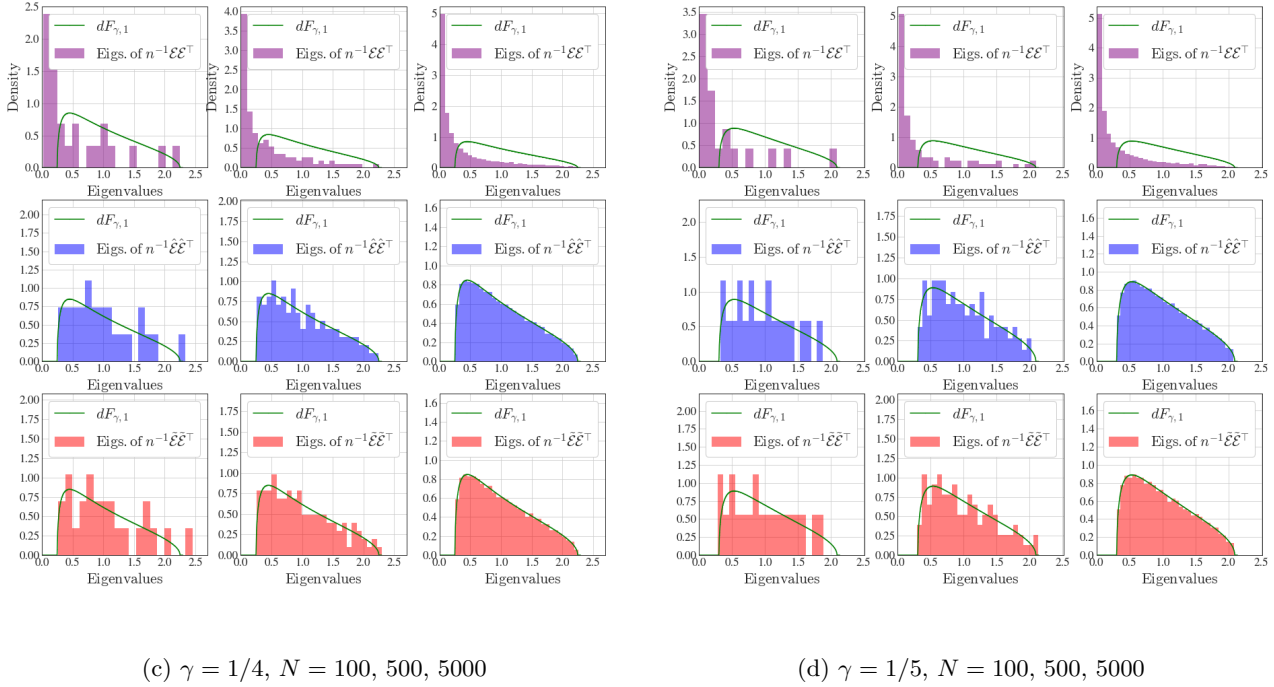
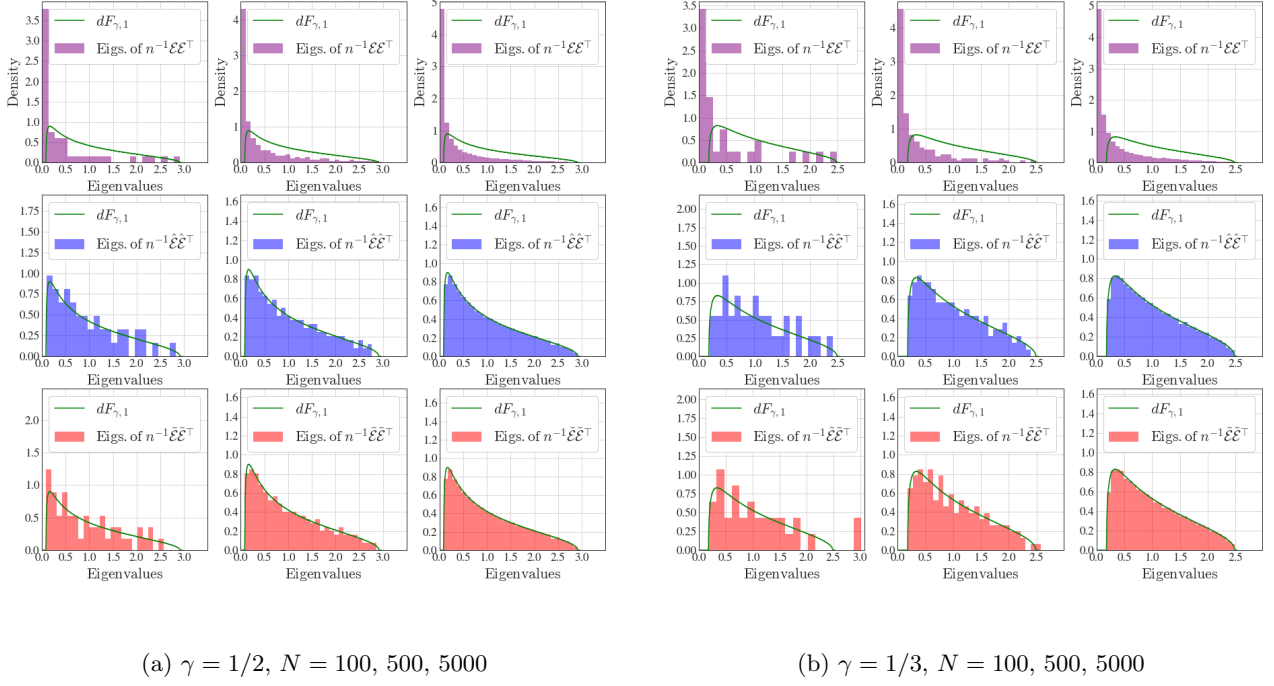


Figure 10: Spectrum of simulated Generalized Poisson noise versus the standard ($\sigma = 1$) Marchenko-Pastur density $dF_{\gamma,1}$, for various aspect ratios γ and matrix dimensions $n = 100, 500, 5000$ (from left to right in each panel). The top row in each panel (purple) corresponds to the eigenvalues of Σ_n (i.e., without any row or column scaling). The center row in each panel (blue) corresponds to the eigenvalues of $\hat{\Sigma}_n$ (i.e., after scaling with the estimated scaling factors). The bottom row in each panel (red) correspond to the eigenvalues of $\tilde{\Sigma}_n$ (i.e., after scaling with the true scaling factors)

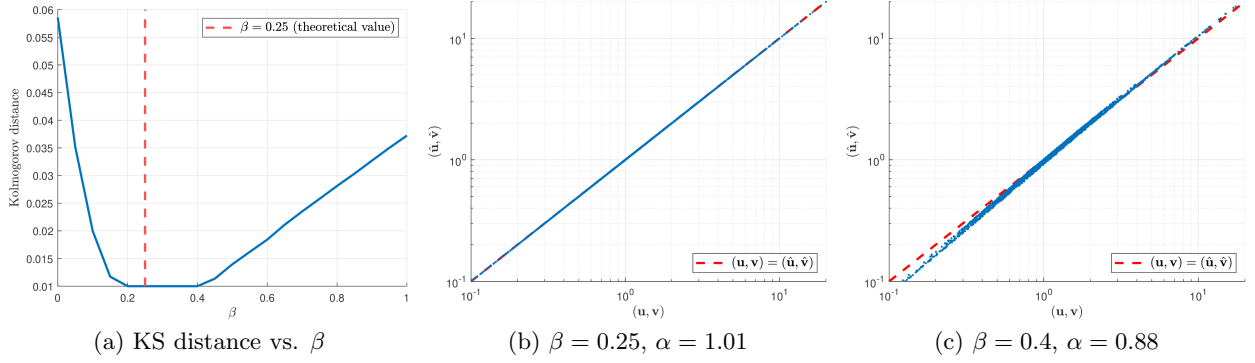


Figure 11: (a) KS distance (26) for $\beta \in \{0, 0.05, \dots, 0.95, 1\}$. (b) Estimated scaling factors $(\hat{\mathbf{u}}, \hat{\mathbf{v}})$ versus the true scaling factors (\mathbf{u}, \mathbf{v}) using the theoretical $\beta = 0.25$ and α chosen by (24). (c) Estimated scaling factors $(\hat{\mathbf{u}}, \hat{\mathbf{v}})$ versus the true scaling factors (\mathbf{u}, \mathbf{v}) using $\beta = 0.4$ (the value furthest away from $\beta = 0.25$ that attains the minimal KS distance of 0.01) and α chosen by (24).

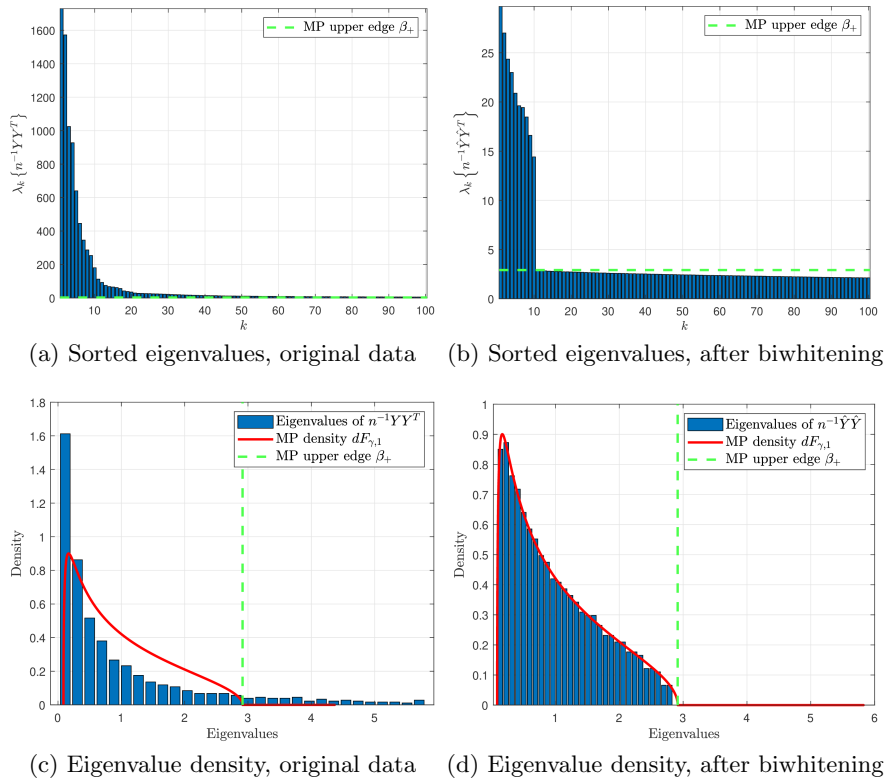


Figure 12: The spectrum of a simulated negative binomial matrix Y with $m = 1000$, $n = 2000$, and $r = 10$, versus the spectrum of its biwhitened version $D(\hat{\mathbf{u}})YD(\hat{\mathbf{v}})$. The number of negative binomial failures was set to 3. To find $\hat{\mathbf{u}}$ and $\hat{\mathbf{v}}$ we solved (17) with the variance estimator (23), where $\beta = 0.4$ and α was chosen according to (24).

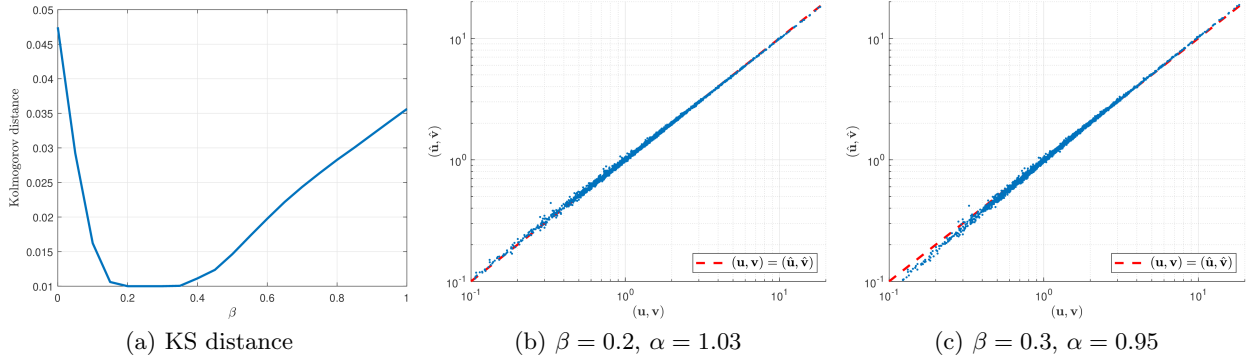


Figure 13: (a) KS distance (26) for $\beta \in \{0, 0.05, \dots, 0.95, 1\}$. (b) Estimated scaling factors $(\hat{\mathbf{u}}, \hat{\mathbf{v}})$ versus the true scaling factors (\mathbf{u}, \mathbf{v}) using $\beta = 0.2$ and α chosen by (24). (c) Estimated scaling factors $(\hat{\mathbf{u}}, \hat{\mathbf{v}})$ versus the true scaling factors (\mathbf{u}, \mathbf{v}) using $\beta = 0.3$ and α chosen by (24).

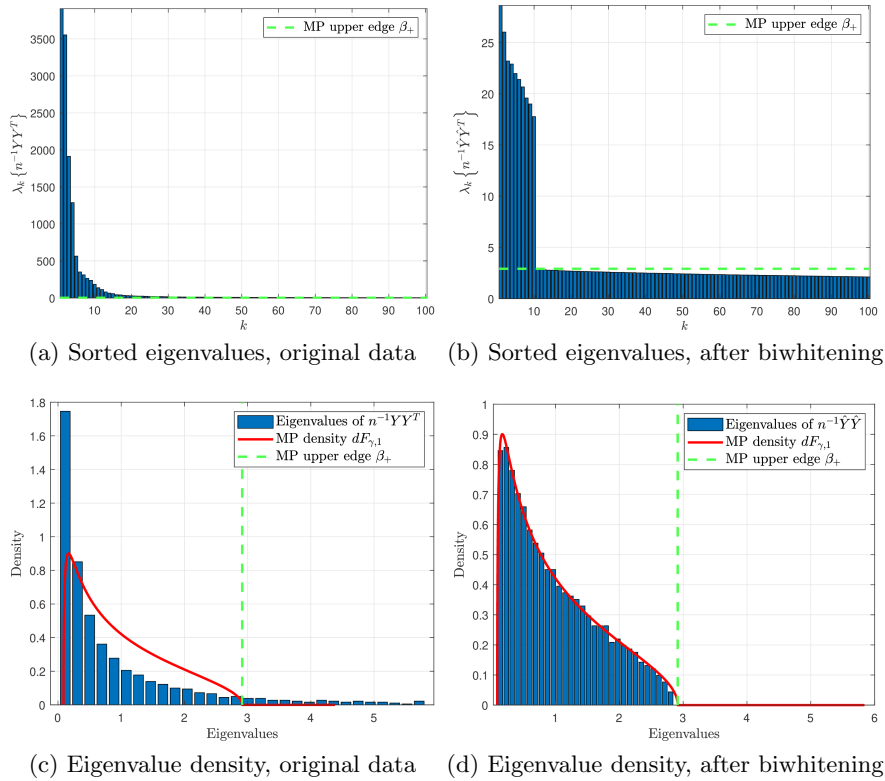


Figure 14: The spectrum of a simulated negative binomial matrix Y with $m = 1000$, $n = 2000$, and $r = 10$, versus the spectrum of its biwhitened version $D(\hat{\mathbf{u}})YD(\hat{\mathbf{v}})$. The number of negative binomial failures for each entry was sampled uniformly at random from $\{1, \dots, 10\}$. To find $\hat{\mathbf{u}}$ and $\hat{\mathbf{v}}$ we solved (17) with the variance estimator (23), where $\beta = 0.3$ and α was chosen according to (24).

for all $i \in [m_n]$ and $j \in [n]$. According to the assumptions in Theorem 2 we have $\max_{i,j} X_{i,j}^{(n)} \leq C \min_{i,j} X_{i,j}^{(n)}$, and therefore (30) asserts that

$$\frac{1}{C^2 \min_{i,j} X_{i,j}^{(n)}} \leq \frac{\min_{i,j} X_{i,j}^{(n)}}{\left(\max_{i,j} X_{i,j}^{(n)}\right)^2} \leq (u_i^{(n)})^2 (v_j^{(n)})^2 \leq \frac{\max_{i,j} X_{i,j}^{(n)}}{\left(\min_{i,j} X_{i,j}^{(n)}\right)^2} \leq \frac{C^2}{\max_{i,j} X_{i,j}^{(n)}}, \quad (31)$$

for all $i \in [m_n]$ and $j \in [n]$.

We now provide an upper bound on the moments of $\tilde{\mathcal{E}}_{i,j}^{(n)}$. We can write

$$\mathbb{E} \left[|\tilde{\mathcal{E}}_{i,j}^{(n)}|^k \right] = \mathbb{E} \left[u_i^k |\mathcal{E}_{i,j}^{(n)}|^k v_j^k \right] \leq \left(\frac{C^2}{\max_{i,j} X_{i,j}^{(n)}} \right)^{k/2} \mathbb{E} \left[|\mathcal{E}_{i,j}^{(n)}|^k \right]. \quad (32)$$

Recall that $\mathbb{E}[\mathcal{E}_{i,j}^{(n)k}]$ is the k 'th central moment of the binomial variable $Y_{i,j}$. According to eq. (4.16) in [42], for all $k \geq 2$ we have the recurrence relation

$$\mathbb{E}[(\mathcal{E}_{i,j}^{(n)})^k] = X_{i,j}^{(n)} \sum_{\ell=0}^{k-2} \binom{k-1}{\ell} \mathbb{E}[(\mathcal{E}_{i,j}^{(n)})^\ell]. \quad (33)$$

Therefore, using the fact that $\mathbb{E}[\mathcal{E}_{i,j}^{(n)}] = 0$, it follows by induction that for all $k = 2, 3, \dots, \infty$

$$\mathbb{E}[(\mathcal{E}_{i,j}^{(n)})^k] = \sum_{\ell=1}^{\lfloor k/2 \rfloor} a_\ell^{(k)} (X_{i,j}^{(n)})^\ell, \quad (34)$$

for some constant coefficients $\{a_\ell^{(k)}\}_{\ell=1}^{\lfloor k/2 \rfloor}$. Hence, for even values of k we can write

$$\begin{aligned} \mathbb{E} \left[|\tilde{\mathcal{E}}_{i,j}^{(n)}|^k \right] &\leq \left(\frac{C^2}{\max_{i,j} X_{i,j}^{(n)}} \right)^{k/2} \mathbb{E} \left[(\mathcal{E}_{i,j}^{(n)})^k \right] \\ &\leq C^k \sum_{\ell=1}^{k/2} a_\ell^{(k)} \frac{(X_{i,j}^{(n)})^\ell}{\max_{i,j} (X_{i,j}^{(n)})^{k/2}} \leq C^k \sum_{\ell=1}^{k/2} a_\ell^{(k)} c^{\ell-k/2}, \end{aligned} \quad (35)$$

where we used the fact that $\max_{i,j} X_{i,j}^{(n)} > c$ for all n . Eventually, for all values of k and n we have

$$\mathbb{E} \left[|\tilde{\mathcal{E}}_{i,j}^{(n)}|^k \right] \leq \sqrt{\mathbb{E}[|\tilde{\mathcal{E}}_{i,j}^{(n)}|^{2k}]} \leq C^k \sqrt{\sum_{\ell=1}^k a_\ell^{(k)} c^{\ell-k}} := \tilde{C}_k. \quad (36)$$

To prove the MP law, we apply Theorem 8.2 in [27] to the matrix $\xi^{(n)} = n^{-1/2} \tilde{\mathcal{E}}^{(n)}$. To that end, note that the entries of $\xi^{(n)} = (n^{-1/2} \tilde{\mathcal{E}}_{i,j}^{(n)})_{i \in [m_n], j \in [n]}$ are independent, and $\xi^{(n)}$ satisfies $\sum_{i=1}^{m_n} \xi_{i,j}^{(n)} = m_n/n$, $\sum_{j=1}^n \xi_{i,j}^{(n)} = 1$ for all $i \in [m_n]$ and $j \in [n]$. We now establish the required Lindeberg condition. Observe that

$$\begin{aligned} \mathbb{E} \left[(\xi_{i,j}^{(n)})^2 \mathbb{1}(|\xi_{i,j}^{(n)}| > \tau) \right] &= \frac{1}{n} \mathbb{E} \left[(\tilde{\mathcal{E}}_{i,j}^{(n)})^2 \mathbb{1}(|\tilde{\mathcal{E}}_{i,j}^{(n)}| > \tau\sqrt{n}) \right] = \frac{1}{n} \int_{|t| > \tau\sqrt{n}} t^2 d\mu_{\tilde{\mathcal{E}}_{i,j}^{(n)}}(t) \\ &< \frac{1}{n} \int_{|t| > \tau\sqrt{n}} \frac{t^4}{\tau^2 n^2} d\mu_{\tilde{\mathcal{E}}_{i,j}^{(n)}}(t) \leq \frac{1}{\tau^2 n^2} \mathbb{E}[(\tilde{\mathcal{E}}_{i,j}^{(n)})^4] \leq \frac{\tilde{C}_4}{\tau^2 n^2}, \end{aligned} \quad (37)$$

where $d\mu_{\tilde{\mathcal{E}}_{i,j}^{(n)}}$ is the probability density of $\tilde{\mathcal{E}}_{i,j}^{(n)}$, and we used (36) to get the last inequality. We then have

$$\begin{aligned} &\lim_{n \rightarrow \infty} \max_{i \in [m_n], j \in [n]} \left[\sum_{j=1}^n \mathbb{E} \left[(\xi_{i,j}^{(n)})^2 \mathbb{1}(|\xi_{i,j}^{(n)}| > \tau) \right] + \sum_{i=1}^{m_n} \mathbb{E} \left[(\xi_{i,j}^{(n)})^2 \mathbb{1}(|\xi_{i,j}^{(n)}| > \tau) \right] \right] \\ &< \lim_{n \rightarrow \infty} \max_{i \in [m_n], j \in [n]} \left[\frac{\tilde{C}_4}{\tau^2} \left(\frac{1}{n} + \frac{m_n}{n^2} \right) \right] = 0, \end{aligned} \quad (38)$$

for every $\tau > 0$. Then, according to Theorem 8.2 in [27], we have almost surely for all τ that

$$\lim_{n \rightarrow \infty} \left| F_{\tilde{\Sigma}^{(n)}}(\tau) - F_{\frac{m_n}{n}, 1}(\tau) \right| = \lim_{n \rightarrow \infty} \left| F_{\tilde{\Sigma}^{(n)}}(\tau) - F_{\gamma, 1}(\tau) \right| = 0. \quad (39)$$

We note that Theorem 8.2 in [27] is actually stated in terms of a distribution associated with the solution to a certain Dyson equation. To see that this distribution is in fact the MP distribution, we refer the reader to [55] where the same equation is analyzed and is shown to provide the distribution whose density has the explicit form (3).

Next, to prove the convergence of the largest eigenvalue to β_+ , we apply Theorem 2.4 part II in [1] to the matrix $\xi^{(n)} = n^{-1/2} \tilde{\mathcal{E}}^{(n)}$ (as X in [1]). To that end, we need to show that the Conditions (A) – (D) in [1] hold, which we consider next. To show Condition (A) in [1], we have

$$\mathbb{E}[(\xi_{i,j}^{(n)})^2] = \frac{\mathbb{E}[(\tilde{\mathcal{E}}_{i,j}^{(n)})^2]}{n} \leq \frac{\tilde{C}_2}{n} \leq \left(\frac{\tilde{C}_2}{n + m_n} \right) \left(1 + \frac{m_n}{n} \right) \leq \frac{\tilde{C}_2(1 + 2\gamma)}{n + m_n}, \quad (40)$$

for all sufficiently large n , where we also used (36). To show Condition (B) in [1], observe that

$$\mathbb{E}[(\xi_{i,j}^{(n)})^2] = \frac{\mathbb{E}[(\tilde{\mathcal{E}}_{i,j}^{(n)})^2]}{n} = \frac{(u_i^{(n)})^2 (v_j^{(n)})^2 X_{i,j}^{(n)}}{n} \geq \frac{X_{i,j}^{(n)}}{nC^2 \min_{i,j} X_{i,j}^{(n)}} \geq \frac{1}{nC^2} \geq \frac{C^{-2}(1 + 0.5\gamma)}{n + m_n}, \quad (41)$$

for all sufficiently large n , where we also used (31). Note that (41) immediately establishes Condition (B) as explained in Remark 2.8 in [1]. Last, Condition (C) in [1] follows by combining (41) with (36), and Condition (D) in [1] follows from our asymptotic setting where $m_n/n \rightarrow \gamma$.

Then, according to Theorem 2.4 part II in [1],

$$\Pr \left\{ \lambda_1 \{ n^{-1} \tilde{\mathcal{E}}^{(n)} (\tilde{\mathcal{E}}^{(n)})^T \} > \beta_+ + \varepsilon_* \right\} \rightarrow 0, \quad (42)$$

for any $\varepsilon_* > 0$, where β_+ is the upper edge of the support of the MP density (3). We mention that Theorem 2.4 part II in [1] is actually stated in terms of the support of a density satisfying an appropriate Dyson equation. To see that this density is in fact the MP density, see the short proof of Theorem 8.2 in [27], where it is shown that the Dyson equation that governs the case of general variances reduces to the Dyson equation giving rise to the MP density if the average variance in each row and in each column of the random matrix is 1.

Last, since the limiting spectral distribution of $n^{-1} \tilde{\mathcal{E}}^{(n)} (\tilde{\mathcal{E}}^{(n)})^T$, given by $F_{\tilde{\Sigma}^{(n)}}(\tau)$, converges almost surely to the MP distribution $F_{\gamma, 1}(\tau)$, which is strictly positive for any $\tau \in (\beta_-, \beta_+)$, then we also have that

$$\Pr \left\{ \lambda_1 \{ n^{-1} \tilde{\mathcal{E}}^{(n)} (\tilde{\mathcal{E}}^{(n)})^T \} < \beta_+ - \varepsilon_* \right\} \rightarrow 0, \quad (43)$$

for any $\varepsilon_* > 0$, which together with (42) establishes that $\lambda_1 \{ \tilde{\Sigma}^{(n)} \} \xrightarrow{P} \beta_+ = (1 + \sqrt{\gamma})^2$.

Appendix G Proof of Theorem 3

Suppose in negation that $\Pr \{ r^{(n)} < \tilde{r}_\varepsilon^{(n)} \}$ does not converge to 0 as $n \rightarrow \infty$. Then, there exists a sequence $\{n_k\}_{k \geq 1}$ with $n_k \xrightarrow[k \rightarrow \infty]{} \infty$ and a constant $\beta > 0$, such that

$$\Pr \{ r^{(n_k)} < \tilde{r}_\varepsilon^{(n_k)} \} \geq \beta, \quad (44)$$

for all $k \geq 1$. In addition, according to the definition of $\tilde{r}_\varepsilon^{(n)}$ we have

$$\lambda_{\tilde{r}_\varepsilon^{(n_k)}} \{ n_k^{-1} \tilde{Y}^{(n_k)} (\tilde{Y}^{(n_k)})^T \} > \left(1 + \sqrt{\frac{m_{n_k}}{n_k}} \right)^2 + \varepsilon, \quad (45)$$

for all $k \geq 1$. We can now write

$$\begin{aligned} 0 < \beta &\leq \Pr \{ r^{(n_k)} < \tilde{r}_\varepsilon^{(n_k)} \} = \Pr \{ r^{(n_k)} + 1 \leq \tilde{r}_\varepsilon^{(n_k)} \} \\ &\leq \Pr \left\{ \lambda_{\tilde{r}_\varepsilon^{(n_k)}} \{ n_k^{-1} \tilde{Y}^{(n_k)} (\tilde{Y}^{(n_k)})^T \} \leq \lambda_{r^{(n_k)} + 1} \{ n_k^{-1} \tilde{Y}^{(n_k)} (\tilde{Y}^{(n_k)})^T \} \right\} \\ &\leq \Pr \left\{ \left(1 + \sqrt{\frac{m_{n_k}}{n_k}} \right)^2 + \varepsilon < \lambda_{r^{(n_k)} + 1} \{ n_k^{-1} \tilde{Y}^{(n_k)} (\tilde{Y}^{(n_k)})^T \} \right\}. \end{aligned} \quad (46)$$

According to Theorem 3.3.16 in [37] we have

$$\sigma_{r^{(n_k)}+1}\{\tilde{Y}^{(n)}\} = \sigma_{r^{(n_k)}+1}\{\tilde{X}^{(n_k)} + \tilde{\mathcal{E}}^{(n_k)}\} \leq \sigma_{r^{(n_k)}+1}\{\tilde{X}^{(n_k)}\} + \sigma_1\{\mathcal{E}^{(n_k)}\} = \sigma_1\{\mathcal{E}^{(n_k)}\}, \quad (47)$$

where $\sigma_i\{\tilde{Y}\}$ is the i 'th largest singular value of \tilde{Y} , and we used the fact that $\text{rank}\{\tilde{X}^{(n_k)}\} = \text{rank}\{X^{(n_k)}\} = r^{(n_k)}$. Therefore, we have

$$\lambda_{r^{(n_k)}+1}\{n_k^{-1}\tilde{Y}^{(n_k)}(\tilde{Y}^{(n_k)})^T\} = n_k^{-1}(\sigma_{r^{(n_k)}+1}\{\tilde{Y}^{(n_k)}\})^2 \leq n_k^{-1}(\sigma_1\{\mathcal{E}^{(n_k)}\})^2 = \|\tilde{\Sigma}^{(n_k)}\|_2. \quad (48)$$

Combining the above with (46) we obtain

$$0 < \beta \leq \Pr\left\{\left(1 + \sqrt{\frac{m_{n_k}}{n_k}}\right)^2 + \varepsilon < \|\tilde{\Sigma}^{(n_k)}\|_2\right\} \leq \Pr\left\{(1 + \sqrt{\gamma})^2 + \frac{\varepsilon}{2} < \|\tilde{\Sigma}^{(n_k)}\|_2\right\}, \quad (49)$$

for all sufficiently large k , where we used the fact that $m_{n_k}/n_k \rightarrow \gamma$. However, from Theorem 2 we know that $\Pr\{\|\tilde{\Sigma}^{(n_k)}\|_2 > \varepsilon/2 + (1 + \sqrt{\gamma})^2\} \rightarrow 0$ as $n \rightarrow \infty$ for any $\varepsilon > 0$, which is a contradiction to (49).

Appendix H Proof of Lemma 4

To prove Lemma 4, we rely on Theorem 3 in [48]. However, since this theorem requires a random matrix with bounded variables (from above and from below away from zero), we define a truncated version of $Y_{i,j} \sim \text{Poisson}(X_{i,j})$ that retains its mean as follows. For any m and n , let $\alpha > 0$, and define the random variable $\{\bar{Y}_{i,j}\}_{i \in [m], j \in [n]}$ according to

$$(\bar{Y}_{i,j}|Y_{i,j} = y) = \begin{cases} y, & X_{i,j}/\alpha \leq y \leq \alpha X_{i,j}, \\ X_{i,j} \frac{\Pr\{Y_{i,j} < X_{i,j}/\alpha - 1\}}{\Pr\{Y_{i,j} < X_{i,j}/\alpha\}}, & y < X_{i,j}/\alpha \\ X_{i,j} \frac{\Pr\{Y_{i,j} > \alpha X_{i,j} - 1\}}{\Pr\{Y_{i,j} > \alpha X_{i,j}\}}, & y > \alpha X_{i,j}. \end{cases} \quad (50)$$

We then have the following lemma.

Lemma 13. $\{\bar{Y}_{i,j}\}_{i \in [m], j \in [n]}$ are independent random variables with $\mathbb{E}[\bar{Y}_{i,j}] = X_{i,j}$, and

$$\min\left\{\frac{1}{\alpha}, 1 - \frac{X_{i,j}}{X_{i,j} + \lceil X_{i,j}/\alpha \rceil - 1}\right\} \leq \frac{\bar{Y}_{i,j}}{X_{i,j}} \leq 1 + \alpha + X_{i,j}^{-1}. \quad (51)$$

Proof. The fact that $\bar{Y}_{i,j}$ are independent follows from their definition. We now prove that $\mathbb{E}[\bar{Y}_{i,j}] = X_{i,j}$. We can write

$$\begin{aligned} \mathbb{E}[\bar{Y}_{i,j}] &= \sum_{k=\lceil X_{i,j}/\alpha \rceil}^{\lfloor \alpha X_{i,j} \rfloor} k \Pr\{Y_{i,j} = k\} + X_{i,j} \Pr\{Y_{i,j} < X_{i,j}/\alpha - 1\} + X_{i,j} \Pr\{Y_{i,j} > \alpha X_{i,j} - 1\} \\ &= \sum_{k=0}^{\infty} k \Pr\{Y_{i,j} = k\} - \sum_{k=0}^{\lceil X_{i,j}/\alpha \rceil - 1} k \Pr\{Y_{i,j} = k\} - \sum_{k=\lfloor \alpha X_{i,j} \rfloor + 1}^{\infty} k \Pr\{Y_{i,j} = k\} \\ &\quad + X \Pr\{Y_{i,j} < X_{i,j}/\alpha - 1\} + X \Pr\{Y_{i,j} > \alpha X_{i,j} - 1\} \\ &= X_{i,j} - \sum_{k=1}^{\lceil X_{i,j}/\alpha \rceil - 1} \frac{X_{i,j}^k e^{-X_{i,j}}}{(k-1)!} - \sum_{k=\lfloor \alpha X_{i,j} \rfloor + 1}^{\infty} \frac{X_{i,j}^k e^{-X_{i,j}}}{(k-1)!} \\ &\quad + X_{i,j} \Pr\{Y_{i,j} < X_{i,j}/\alpha - 1\} + X_{i,j} \Pr\{Y_{i,j} > \alpha X_{i,j} - 1\} \\ &= X_{i,j} - X_{i,j} \sum_{k=0}^{\lceil X_{i,j}/\alpha \rceil - 2} \Pr\{Y_{i,j} = k\} - X_{i,j} \sum_{k=\lfloor \alpha X_{i,j} \rfloor}^{\infty} \Pr\{Y_{i,j} = k\} \\ &\quad + X_{i,j} \Pr\{Y_{i,j} < X_{i,j}/\alpha - 1\} + X_{i,j} \Pr\{Y_{i,j} > \alpha X_{i,j} - 1\} \\ &= X_{i,j}. \end{aligned} \quad (52)$$

To show (51), observe that

$$\begin{aligned}
X_{i,j} &\geq X_{i,j} \frac{\Pr\{Y < X_{i,j}/\alpha - 1\}}{\Pr\{Y < X_{i,j}/\alpha\}} = X_{i,j} \frac{\Pr\{Y < X_{i,j}/\alpha\} - \Pr\{Y = \lceil X_{i,j}/\alpha \rceil - 1\}}{\Pr\{Y < X_{i,j}/\alpha\}} \\
&= X_{i,j} \left(1 - \frac{\Pr\{Y = \lceil X_{i,j}/\alpha \rceil - 1\}}{\Pr\{Y < X_{i,j}/\alpha\}} \right) \geq X_{i,j} \left(1 - \frac{\Pr\{Y = \lceil X_{i,j}/\alpha \rceil - 1\}}{\Pr\{Y = \lceil X_{i,j}/\alpha \rceil - 1\} + \Pr\{Y = \lceil X_{i,j}/\alpha \rceil - 2\}} \right) \\
&= X_{i,j} \left(1 - \frac{\Pr\{Y = \lceil X_{i,j}/\alpha \rceil - 1\}}{\Pr\{Y = \lceil X_{i,j}/\alpha \rceil - 1\} (1 + (\lceil X_{i,j}/\alpha \rceil - 1)/X_{i,j})} \right) = X_{i,j} \left(1 - \frac{X_{i,j}}{X_{i,j} + \lceil X_{i,j}/\alpha \rceil - 1} \right), \tag{53}
\end{aligned}$$

where we used the property of the Poisson distribution $\Pr\{Y_{i,j} = k\} = \Pr\{Y_{i,j} = k + 1\}(k + 1)/X_{i,j}$ (which follows immediately from its probability-mass function). Similarly, we have

$$\begin{aligned}
X_{i,j} &\leq X_{i,j} \frac{\Pr\{Y_{i,j} > \alpha X_{i,j} - 1\}}{\Pr\{Y_{i,j} > \alpha X_{i,j}\}} = X_{i,j} \frac{\Pr\{Y_{i,j} > \alpha X_{i,j}\} + \Pr\{Y_{i,j} = \lfloor \alpha X_{i,j} \rfloor\}}{\Pr\{Y_{i,j} > \alpha X_{i,j}\}} \\
&= X_{i,j} \left(1 + \frac{\Pr\{Y_{i,j} = \lfloor \alpha X_{i,j} \rfloor\}}{\Pr\{Y_{i,j} > \alpha X_{i,j}\}} \right) \leq X_{i,j} \left(1 + \frac{\Pr\{Y_{i,j} = \lfloor \alpha X_{i,j} \rfloor + 1\}(\lfloor \alpha X_{i,j} \rfloor + 1)/X_{i,j}}{\Pr\{Y_{i,j} > \alpha X_{i,j}\}} \right) \\
&< X_{i,j} \left(1 + \frac{\lfloor \alpha X_{i,j} \rfloor + 1}{X_{i,j}} \right) \leq X_{i,j} (1 + \alpha + X_{i,j}^{-1}), \tag{54}
\end{aligned}$$

where we used the fact that $\Pr\{Y = \lfloor \alpha X_{i,j} \rfloor + 1\} < \Pr\{Y > \alpha X_{i,j}\}$, and again the property $\Pr\{Y_{i,j} = k\} = \Pr\{Y_{i,j} = k + 1\}(k + 1)/X_{i,j}$. Combining (54) and (53) together with the definition of $\bar{Y}_{i,j}$ proves (51). \square

Now, let $\bar{Y}_{i,j}^{(n)}$ be as in (50) when replacing $Y_{i,j}$ and $X_{i,j}$ with $Y_{i,j}^{(n)}$ and $X_{i,j}^{(n)}$, respectively. Observe that since $X_{i,j}^{(n)} \rightarrow \infty$ as $n \rightarrow \infty$ (by the conditions in Lemma 4) and according to (51), for any $\alpha > 0$ there exist constants $0 < \alpha_1 \leq \alpha_2$ such that for all sufficiently large n :

$$\alpha_1 X_{i,j}^{(n)} \leq \bar{Y}_{i,j}^{(n)} \leq \alpha_2 X_{i,j}^{(n)}. \tag{55}$$

Next we will show that $\bar{Y}_{i,j}^{(n)} = Y_{i,j}^{(n)}$ for all $i \in [m]$ and $j \in [n]$ with probability tending 1 as $n \rightarrow \infty$. To that end, according to Proposition 11.15 in [28], each variable $Y_{i,j} \sim \text{Poisson}(X_{i,j})$ admits the following sub-exponential tail bound:

$$\Pr\{|Y_{i,j} - X_{i,j}| \geq t\} \leq \exp\left(-c' \frac{t^2}{X_{i,j} + t}\right), \tag{56}$$

for all $t > 0$ and some universal constant $c' > 0$. For any index n , taking $t = (\alpha - 1)X_{i,j}^{(n)}$ for $\alpha > 1$ gives

$$\Pr\{Y_{i,j}^{(n)} \geq \alpha X_{i,j}^{(n)}\} \leq \exp\left(-\frac{c'(\alpha - 1)^2 X_{i,j}^{(n)}}{\alpha}\right) \leq \exp\left(-\frac{cc'(\alpha - 1)^2}{C\alpha}(\log n)^{1+\epsilon}\right). \tag{57}$$

where we used the fact that $c(\log n)^{1+\epsilon} \leq \max_{i,j} X_{i,j}^{(n)} \leq C \min_{i,j} X_{i,j}^{(n)}$. Analogously, taking $t = (1 - \alpha^{-1})X_{i,j}^{(n)}$ for $\alpha > 1$ gives

$$\Pr\{Y_{i,j}^{(n)} \leq \frac{X_{i,j}^{(n)}}{\alpha}\} \leq \exp\left(-\frac{c'(1 - \alpha^{-1})^2}{2 - \alpha^{-1}} X_{i,j}^{(n)}\right) \leq \exp\left(-\frac{c'(1 - \alpha^{-1})^2}{C(2 - \alpha^{-1})}(\log n)^{1+\epsilon}\right). \tag{58}$$

Therefore, using the union bound and the fact that $m_n/n \rightarrow \gamma$ we have that

$$\begin{aligned}
\Pr\{\bar{Y}^{(n)} \neq Y^{(n)}\} &= \Pr\left\{\bigcup_{i,j} \{\bar{Y}_{i,j}^{(n)} \neq Y_{i,j}^{(n)}\}\right\} \\
&\leq \sum_{i \in [m_n], j \in [n]} \left[\Pr\{Y_{i,j}^{(n)} \geq \alpha X_{i,j}^{(n)}\} + \Pr\{Y_{i,j}^{(n)} \leq \frac{X_{i,j}^{(n)}}{\alpha}\} \right] \tag{59}
\end{aligned}$$

$$\leq m_n n \left[\exp\left(-\frac{cc'(\alpha - 1)^2}{C\alpha}(\log n)^{1+\epsilon}\right) + \exp\left(-\frac{c'(1 - \alpha^{-1})^2}{C(2 - \alpha^{-1})}(\log n)^{1+\epsilon}\right) \right] \xrightarrow{n \rightarrow \infty} 0. \tag{60}$$

We can now apply Theorem 3 in [48] to the random matrix $\bar{Y}^{(n)} = (\bar{Y}_{i,j}^{(n)})_{i \in [m_n], j \in [n]}$ for sufficiently large n using the bounds in (55). Then, together with (60) it follows that for any $\delta \in (0, 1]$, with probability at least

$$1 - 2m_n \exp\left(-\frac{\delta^2 n}{C_p^2}\right) - 2n \exp\left(-\frac{\delta^2 m_n}{C_p^2}\right) - \Pr\left\{\bar{Y}^{(n)} \neq Y^{(n)}\right\}, \quad (61)$$

there exists a pair of positive random vectors $(\tilde{\mathbf{x}}^{(n)}, \tilde{\mathbf{y}}^{(n)})$ that scales $Y^{(n)}$ to row sums n and column sums m_n , such that for all i, j :

$$\frac{|\tilde{x}_i^{(n)} - (u_i^{(n)})^2|}{(u_i^{(n)})^2} \leq C_e \delta, \quad \frac{|\tilde{y}_j^{(n)} - (v_j^{(n)})^2|}{(v_j^{(n)})^2} \leq C_e \delta, \quad (62)$$

where

$$C_p = \sqrt{2} \left(\frac{\alpha_2}{\alpha_1}\right)^2, \quad C_e = 1 + 2 \left(\frac{\alpha_2}{\alpha_1}\right)^{7/2}. \quad (63)$$

Taking any $\alpha > 1$ and $\delta = C_p \sqrt{2 \max\{1, \gamma^{-1}\} \log n/n}$, we obtain that there exists $C' > 0$ such that

$$\frac{|\tilde{x}_i^{(n)} - (u_i^{(n)})^2|}{(u_i^{(n)})^2} \leq C' \sqrt{\frac{\log n}{n}}, \quad \frac{|\tilde{y}_j^{(n)} - (v_j^{(n)})^2|}{(v_j^{(n)})^2} \leq C' \sqrt{\frac{\log n}{n}}, \quad (64)$$

for all i, j , with probability that tends to 1 as $n \rightarrow \infty$. Note that we can always find a constant $a_n > 0$ such that $\tilde{x}_i^{(n)} = a_n^2 (\hat{u}_i^{(n)})^2$ and $\tilde{y}_j^{(n)} = a_n^{-2} (\hat{v}_j^{(n)})^2$ for all i, j . Therefore, we have

$$\left| \left(\frac{a_n \hat{u}_i^{(n)}}{u_i^{(n)}}\right)^2 - 1 \right| \leq C' \sqrt{\frac{\log n}{n}}, \quad \left| \left(\frac{a_n^{-1} \hat{v}_j^{(n)}}{v_j^{(n)}}\right)^2 - 1 \right| \leq C' \sqrt{\frac{\log n}{n}}, \quad (65)$$

for all i, j , with probability that tends to 1 as $n \rightarrow \infty$. Using the Taylor expansion of the function $\sqrt{1 + \varepsilon}$ around $\varepsilon = 0$, we get

$$\left| \frac{a_n \hat{u}_i^{(n)}}{u_i^{(n)}} - 1 \right| \leq \tilde{C} \sqrt{\frac{\log n}{n}}, \quad \left| \frac{a_n^{-1} \hat{v}_j^{(n)}}{v_j^{(n)}} - 1 \right| \leq \tilde{C} \sqrt{\frac{\log n}{n}}, \quad (66)$$

for all i, j and some constant $\tilde{C} > 0$, with probability that tends to 1 as $n \rightarrow \infty$.

Appendix I Proof of Theorem 5

Let us denote $\mathbf{e}_1^{(n)} = a_n \hat{\mathbf{u}}^{(n)} - \mathbf{u}^{(n)}$ and $\mathbf{e}_2^{(n)} = a_n^{-1} \hat{\mathbf{v}}^{(n)} - \mathbf{v}^{(n)}$. We can now write

$$\begin{aligned} \frac{1}{\sqrt{n}} \|\tilde{\mathcal{E}}^{(n)} - \hat{\mathcal{E}}^{(n)}\|_2 &= \frac{1}{\sqrt{n}} \|D(\mathbf{u}^{(n)})\mathcal{E}^{(n)}D(\mathbf{v}^{(n)}) - D(\hat{\mathbf{u}}^{(n)})\mathcal{E}^{(n)}D(\hat{\mathbf{v}}^{(n)})\|_2 \\ &= \frac{1}{\sqrt{n}} \|D(\mathbf{u}^{(n)})\mathcal{E}^{(n)}D(\mathbf{v}^{(n)}) - D(a_n \hat{\mathbf{u}}^{(n)})\mathcal{E}^{(n)}D(a_n^{-1} \hat{\mathbf{v}}^{(n)})\|_2 \\ &\leq \frac{1}{\sqrt{n}} \|D(\mathbf{u}^{(n)})\mathcal{E}^{(n)}D(\mathbf{e}_2^{(n)})\|_2 + \frac{1}{\sqrt{n}} \|D(\mathbf{e}_1^{(n)})\mathcal{E}^{(n)}D(\mathbf{v}^{(n)})\|_2 + \frac{1}{\sqrt{n}} \|D(\mathbf{e}_1^{(n)})\mathcal{E}^{(n)}D(\mathbf{e}_2^{(n)})\|_2 \\ &\leq \frac{\|\mathcal{E}^{(n)}\|_2}{\sqrt{n}} \left(\|D(\mathbf{u}^{(n)})\|_2 \cdot \|D(\mathbf{e}_2^{(n)})\|_2 + \|D(\mathbf{v}^{(n)})\|_2 \cdot \|D(\mathbf{e}_1^{(n)})\|_2 + \|D(\mathbf{e}_1^{(n)})\|_2 \cdot \|D(\mathbf{e}_2^{(n)})\|_2 \right). \end{aligned} \quad (67)$$

According to Lemma 4 we have

$$\|D(\mathbf{e}_1^{(n)})\|_2 = \max_j |a_n^{-1} \hat{v}_j^{(n)} - v_j^{(n)}| \leq \tilde{C} \sqrt{\frac{\log n}{n}} \max_j v_j^{(n)} \quad (68)$$

$$\|D(\mathbf{e}_2^{(n)})\|_2 = \max_i |a_n \hat{u}_i^{(n)} - u_i^{(n)}| \leq \tilde{C} \sqrt{\frac{\log n}{n}} \max_i u_i^{(n)}, \quad (69)$$

with probability that tends to 1 as $n \rightarrow \infty$. Therefore, substituting (68) and (69) into (67) while utilizing (31) gives

$$\frac{1}{\sqrt{n}} \|\tilde{\mathcal{E}}^{(n)} - \hat{\mathcal{E}}^{(n)}\|_2 \leq \frac{\|\mathcal{E}^{(n)}\|_2}{\sqrt{n}} \left(\frac{2\tilde{C}C^2\sqrt{\log n}}{\sqrt{n \max_{i,j} X_{i,j}^{(n)}}} + \frac{\tilde{C}^2 C^2 \log n}{n \sqrt{\max_{i,j} X_{i,j}^{(n)}}} \right), \quad (70)$$

with probability that tends to 1 as $n \rightarrow \infty$. Since $\{\mathcal{E}_{i,j}^{(n)}\}_{i \in [m_n], j \in [n]}$ are independent, $\mathbb{E}[\mathcal{E}_{i,j}^{(n)}] = 0$, $\mathbb{E}(\mathcal{E}_{i,j}^{(n)})^2 = X_{i,j}^{(n)}$, and $\mathbb{E}(\mathcal{E}_{i,j}^{(n)})^4 = X_{i,j}^{(n)} + 3(X_{i,j}^{(n)})^2$ (see (33)), [50] asserts that

$$\begin{aligned} \mathbb{E}\|\mathcal{E}^{(n)}\|_2 &\leq \tilde{C}_2 \left[\sqrt{n \max_{i,j} X_{i,j}^{(n)}} + \sqrt{m_n \max_{i,j} X_{i,j}^{(n)}} + \left(nm_n \max_{i,j} \{X_{i,j}^{(n)} + 3(X_{i,j}^{(n)})^2\} \right)^{1/4} \right] \\ &\leq \tilde{C}_3 \sqrt{n \max_{i,j} X_{i,j}^{(n)}}, \end{aligned} \quad (71)$$

for all sufficiently large n and some universal constants \tilde{C}_2, \tilde{C}_3 , where we used the fact that $X_{i,j}^{(n)} = (X_{i,j}^{(n)})^2 / X_{i,j}^{(n)} \leq C(X_{i,j}^{(n)})^2 / (c(\log n)^{1+\epsilon})$ and that $m_n/n \rightarrow \gamma$ as $n \rightarrow \infty$. Consequently, applying Markov's inequality gives

$$\|\mathcal{E}^{(n)}\|_2 \leq \log n \sqrt{n \max_{i,j} X_{i,j}^{(n)}}, \quad (72)$$

with probability that tends to 1 as $n \rightarrow \infty$. Combining (72) with (70), we get

$$\frac{1}{\sqrt{n}} \|\tilde{\mathcal{E}}^{(n)} - \hat{\mathcal{E}}^{(n)}\|_2 \leq \tilde{C}_3 \frac{(\log n)^{3/2}}{\sqrt{n}}, \quad (73)$$

for some constant \tilde{C}_3 , with probability that tends to 1 as $n \rightarrow \infty$. Hence, it follows that (see Theorem 3.3.16 in [37])

$$\max_i \left| s_i \left\{ \frac{1}{\sqrt{n}} \tilde{\mathcal{E}}^{(n)} \right\} - s_i \left\{ \frac{1}{\sqrt{n}} \hat{\mathcal{E}}^{(n)} \right\} \right| \leq \tilde{C}_3 \frac{(\log n)^{3/2}}{\sqrt{n}}, \quad (74)$$

with probability that tends to 1 as $n \rightarrow \infty$, where $s_i\{A\}$ is the i 'th largest singular value of A . We then have that

$$\begin{aligned} \max_i \left| \lambda_i \left\{ \frac{1}{n} \tilde{\mathcal{E}}^{(n)} (\tilde{\mathcal{E}}^{(n)})^T \right\} - \lambda_i \left\{ \frac{1}{n} \hat{\mathcal{E}}^{(n)} (\hat{\mathcal{E}}^{(n)})^T \right\} \right| &= \max_i \left| s_i^2 \left\{ \frac{1}{\sqrt{n}} \tilde{\mathcal{E}}^{(n)} \right\} - s_i^2 \left\{ \frac{1}{\sqrt{n}} \hat{\mathcal{E}}^{(n)} \right\} \right| \\ &= \max_i \left\{ \left(s_i \left\{ \frac{1}{\sqrt{n}} \tilde{\mathcal{E}}^{(n)} \right\} + s_i \left\{ \frac{1}{\sqrt{n}} \hat{\mathcal{E}}^{(n)} \right\} \right) \cdot \left| s_i \left\{ \frac{1}{\sqrt{n}} \tilde{\mathcal{E}}^{(n)} \right\} - s_i \left\{ \frac{1}{\sqrt{n}} \hat{\mathcal{E}}^{(n)} \right\} \right| \right\} \\ &\leq \tilde{C}_3 \frac{(\log n)^{3/2}}{\sqrt{n}} \max_i \left\{ s_i \left\{ \frac{1}{\sqrt{n}} \tilde{\mathcal{E}}^{(n)} \right\} + s_i \left\{ \frac{1}{\sqrt{n}} \hat{\mathcal{E}}^{(n)} \right\} \right\} = \tilde{C}_3 \frac{(\log n)^{3/2}}{n} \left(\|\tilde{\mathcal{E}}^{(n)}\|_2 + \|\hat{\mathcal{E}}^{(n)}\|_2 \right), \end{aligned} \quad (75)$$

with probability that tends to 1 as $n \rightarrow \infty$. Using (72) and (31) we have

$$\begin{aligned} \|\tilde{\mathcal{E}}^{(n)}\|_2 &= \|D(\mathbf{u}^{(n)}) \mathcal{E}^{(n)} D(\mathbf{v}^{(n)})\|_2 \leq \|D(\mathbf{u}^{(n)})\|_2 \cdot \|\mathcal{E}^{(n)}\|_2 \cdot \|D(\mathbf{v}^{(n)})\|_2 \\ &\leq \log n \sqrt{n \max_{i,j} X_{i,j}^{(n)}} \max_i u_i^{(n)} \max_j v_j^{(n)} \leq C\sqrt{n} \log n, \end{aligned} \quad (76)$$

with probability that tends to 1 as $n \rightarrow \infty$. Employing the above together with (73) we obtain

$$\|\hat{\mathcal{E}}\|_2 \leq \|\tilde{\mathcal{E}}^{(n)}\|_2 + \|\hat{\mathcal{E}}^{(n)} - \tilde{\mathcal{E}}^{(n)}\|_2 \leq C\sqrt{n} \log n + \tilde{C}_3 (\log n)^{3/2}, \quad (77)$$

with probability that tends to 1 as $n \rightarrow \infty$. Overall, it follows that

$$\max_i \left| \lambda_i \left\{ \frac{1}{n} \tilde{\mathcal{E}}^{(n)} (\tilde{\mathcal{E}}^{(n)})^T \right\} - \lambda_i \left\{ \frac{1}{n} \hat{\mathcal{E}}^{(n)} (\hat{\mathcal{E}}^{(n)})^T \right\} \right| \xrightarrow[n \rightarrow \infty]{p} 0, \quad (78)$$

where \xrightarrow{p} refers to convergence in probability.

Appendix J Proof of Proposition 12

J.1 Proof that A is not completely decomposable

We begin by showing that A is not completely decomposable under the conditions in Proposition 11. To that end, assume in negation that A is completely decomposable. Then, since A does not have any zero rows and columns, there must exist proper nonempty subsets $\mathcal{I}_1 \subset [m]$ and $\mathcal{I}_2 \subset [n]$ such that $[A]_{i \in \mathcal{I}_1, j \in \mathcal{I}_2}$ and $[A]_{i \in \mathcal{I}_1^c, j \in \mathcal{I}_2^c}$ are both zero matrices. We can assume without loss of generality that $|\mathcal{I}_2| \geq n/2$, as otherwise we simply replace $(\mathcal{I}_1, \mathcal{I}_2)$ with $(\mathcal{I}_1^c, \mathcal{I}_2^c)$. Let us define $k = n - |\mathcal{I}_2|$, and since $|\mathcal{I}_2| \geq n/2$, we have that $n \geq 2k$. Now, if $|\mathcal{I}_1| \geq m/2$ we immediately get a contradiction to condition 1 in Proposition 11, since $[A]_{i \in \mathcal{I}_1, j \in \mathcal{I}_2}$ has $|\mathcal{I}_1|$ rows with $|\mathcal{I}_2| = n - k$ zeros each, where

$$|\mathcal{I}_1| \geq \frac{m}{2} = \frac{mk}{n} \frac{n}{2k} \geq \frac{mk}{n}, \quad (79)$$

and we used the fact that $n \geq 2k$. We next consider the alternative possibility that $|\mathcal{I}_1| < m/2$. In this case, we must have that

$$|\mathcal{I}_1| < \frac{mk}{n}, \quad (80)$$

as otherwise we get a contradiction to condition 1 in Proposition 11 (using the fact that $|\mathcal{I}_1|$ is an integer). In addition, the matrix $[A]_{i \in \mathcal{I}_1^c, j \in \mathcal{I}_2^c}$ has $|\mathcal{I}_2^c| = n - |\mathcal{I}_2|$ columns that have $|\mathcal{I}_1^c| = m - |\mathcal{I}_1|$ zeros each. We define $\ell = |\mathcal{I}_1|$, which satisfies $\ell < m/2$. Therefore, we also must have that

$$n - |\mathcal{I}_2| < \frac{n\ell}{m} = \frac{n|\mathcal{I}_1|}{m} < k, \quad (81)$$

as otherwise we get a contradiction to condition 2 in Proposition 11, where we used (80) and the fact that $n - |\mathcal{I}_2|$ is an integer. Overall, recall that $k = n - |\mathcal{I}_2|$, which together with (81) gives $k < k$, a contradiction to our initial assumption that A is completely decomposable.

J.2 Proof that Condition 10 holds

We next prove that that Condition 10 holds. Let us assume in negation that Condition 10 does not hold. Then, since A does not have any zero rows and columns, we must have that

$$|\mathcal{I}_1|n + |\mathcal{I}_2|m \geq mn, \quad (82)$$

for some proper nonempty subsets $\mathcal{I}_1 \subset [m]$ and $\mathcal{I}_2 \subset [n]$ for which $[A]_{i \in \mathcal{I}_1, j \in \mathcal{I}_2}$ is a zero matrix. It follows that either $|\mathcal{I}_2| \geq n/2$ or $|\mathcal{I}_1| \geq m/2$. Suppose that the former holds, that is $|\mathcal{I}_2| \geq n/2$, and define $k = n - |\mathcal{I}_2|$ which satisfies $0 < k \leq n/2$. Observe that the matrix $[A]_{i \in \mathcal{I}_1, j \in \mathcal{I}_2}$ has $|\mathcal{I}_1|$ rows with $|\mathcal{I}_2| = n - k$ zeros each. Using the fact that $|\mathcal{I}_1|n + |\mathcal{I}_2|m \geq mn$ we have

$$|\mathcal{I}_1| \geq \frac{m(n - |\mathcal{I}_2|)}{n} = \frac{mk}{n}, \quad (83)$$

which is a contradiction to condition 1 in Proposition 11 (using the fact that $|\mathcal{I}_1|$ is an integer). We next assume that the other possibility holds, namely that $|\mathcal{I}_1| \geq m/2$, and define $\ell = m - |\mathcal{I}_1|$ which satisfies $0 < \ell \leq m/2$. Observe that the matrix $[A]_{i \in \mathcal{I}_1, j \in \mathcal{I}_2}$ has $|\mathcal{I}_2|$ columns with $|\mathcal{I}_1| = m - \ell$ zeros each. Using the fact that $|\mathcal{I}_1|n + |\mathcal{I}_2|m \geq mn$ we have

$$|\mathcal{I}_2| \geq \frac{n(m - |\mathcal{I}_1|)}{m} = \frac{n\ell}{m}, \quad (84)$$

which is a contradiction to condition 2 in Proposition 11 (using the fact that $|\mathcal{I}_2|$ is an integer). Therefore, we have a contradiction to our assumption that Condition 10 does not hold, thereby concluding the proof.

Appendix K Proof of Proposition 8

The fact that (19) is an unbiased estimator for $\text{Var}[Y_{i,j}]$ follows from direct calculation, as

$$\begin{aligned} \mathbb{E}[\widehat{\text{Var}}[Y_{i,j}]] &= \frac{a + bX_{i,j} + c\mathbb{E}[Y_{i,j}^2]}{1 + c} \\ &= \frac{a + bX_{i,j} + c(a + bX_{i,j} + (c + 1)X_{i,j}^2)}{1 + c} = \text{Var}[Y_{i,j}], \end{aligned} \quad (85)$$

where we used $\mathbb{E}[Y_{i,j}^2] = \text{Var}[Y_{i,j}] + X_{i,j}^2$ together with the QVF property (18). Next, if $Y_{i,j} \sim \text{Bernoulli}(p_{i,j})$ then $\text{Var}[Y_{i,j}] = p_{i,j} - p_{i,j}^2$, hence $c = -1$. Among the six fundamental NEF-QVFs, the binomial is the only family with $c < 0$, and according to the formulas in [57], while the value of c is invariant to linear transformations, it must change under a (non-null) convolution or division. Hence, the case of $c = -1$ corresponds uniquely to a linear transformation of a Bernoulli. Lastly, for any $f : \{0, 1\} \rightarrow \{c_0, c_1\}$ we have $\mathbb{E}[f(Y_{i,j})] = c_0 p_{i,j} + c_1(1 - p_{i,j})$, which is a first degree polynomial in $p_{i,j}$ that cannot possibly match $\text{Var}[Y_{i,j}]$ for all values of $p_{i,j} \in [0, 1]$.

References

- [1] Johannes Alt, László Erdős, Torben Krüger, et al. Local law for random gram matrices. *Electronic Journal of Probability*, 22, 2017.
- [2] Jason Altschuler, Jonathan Weed, and Philippe Rigollet. Near-linear time approximation algorithms for optimal transport via sinkhorn iteration. *arXiv preprint arXiv:1705.09634*, 2017.
- [3] Zhidong Bai and Jack W Silverstein. *Spectral analysis of large dimensional random matrices*, volume 20. Springer, 2010.
- [4] Jinho Baik, Gérard Ben Arous, Sandrine Péché, et al. Phase transition of the largest eigenvalue for nonnull complex sample covariance matrices. *Annals of Probability*, 33(5):1643–1697, 2005.
- [5] Jinho Baik and Jack W Silverstein. Eigenvalues of large sample covariance matrices of spiked population models. *Journal of multivariate analysis*, 97(6):1382–1408, 2006.
- [6] Florent Benaych-Georges and Raj Rao Nadakuditi. The eigenvalues and eigenvectors of finite, low rank perturbations of large random matrices. *Advances in Mathematics*, 227(1):494–521, 2011.
- [7] Jérémie Bigot and Charles Deledalle. Low-rank matrix denoising for count data using unbiased kullback-leibler risk estimation. *arXiv preprint arXiv:2001.10391*, 2020.
- [8] Jérémie Bigot, Charles Deledalle, and Delphine Féral. Generalized sure for optimal shrinkage of singular values in low-rank matrix denoising. *The Journal of Machine Learning Research*, 18(1):4991–5040, 2017.
- [9] Johan Braeken and Marcel ALM Van Assen. An empirical kaiser criterion. *Psychological Methods*, 22(3):450, 2017.
- [10] Richard A Brualdi. The dad theorem for arbitrary row sums. *Proceedings of the American Mathematical Society*, 45(2):189–194, 1974.
- [11] Richard A Brualdi, Seymour V Parter, and Hans Schneider. The diagonal equivalence of a nonnegative matrix to a stochastic matrix. *Journal of Mathematical Analysis and Applications*, 16(1):31–50, 1966.
- [12] Changxiao Cai, Gen Li, Yuejie Chi, H Vincent Poor, and Yuxin Chen. Subspace estimation from unbalanced and incomplete data matrices: $l_{2,\infty}$ statistical guarantees. *arXiv preprint arXiv:1910.04267*, 2019.
- [13] Yang Cao and Yao Xie. Poisson matrix recovery and completion. *IEEE Transactions on Signal Processing*, 64(6):1609–1620, 2015.
- [14] Raymond B Cattell. The scree test for the number of factors. *Multivariate behavioral research*, 1(2):245–276, 1966.
- [15] Deeparnab Chakrabarty and Sanjeev Khanna. Better and simpler error analysis of the sinkhorn-knopp algorithm for matrix scaling. *Mathematical Programming*, pages 1–13, 2020.
- [16] Sourav Chatterjee et al. Matrix estimation by universal singular value thresholding. *Annals of Statistics*, 43(1):177–214, 2015.
- [17] Yunjin Choi, Jonathan Taylor, and Robert Tibshirani. Selecting the number of principal components: Estimation of the true rank of a noisy matrix. *The Annals of Statistics*, pages 2590–2617, 2017.
- [18] Prem C Consul and Gaurav C Jain. A generalization of the poisson distribution. *Technometrics*, 15(4):791–799, 1973.

- [19] Judit Csima and Biswa Nath Datta. The dad theorem for symmetric non-negative matrices. *Journal of Combinatorial Theory, Series A*, 12(1):147–152, 1972.
- [20] Edgar Dobriban et al. Permutation methods for factor analysis and pca. *Annals of Statistics*, 48(5):2824–2847, 2020.
- [21] Edgar Dobriban and Art B Owen. Deterministic parallel analysis: an improved method for selecting factors and principal components. *Journal of the Royal Statistical Society: Series B (Statistical Methodology)*, 81(1):163–183, 2019.
- [22] David L Donoho, Matan Gavish, and Elad Romanov. Screenot: Exact mse-optimal singular value thresholding in correlated noise. *arXiv preprint arXiv:2009.12297*, 2020.
- [23] Jianqing Fan, Jianhua Guo, and Shurong Zheng. Estimating number of factors by adjusted eigenvalues thresholding. *Journal of the American Statistical Association*, pages 1–10, 2020.
- [24] Jianqing Fan, Qiang Sun, Wen-Xin Zhou, and Ziwei Zhu. Principal component analysis for big data. *Wiley StatsRef: Statistics Reference Online*, pages 1–13, 2014.
- [25] Matan Gavish and David L Donoho. The optimal hard threshold for singular values is $4/\sqrt{3}$. *IEEE Transactions on Information Theory*, 60(8):5040–5053, 2014.
- [26] Stuart Geman. A limit theorem for the norm of random matrices. *The Annals of Probability*, pages 252–261, 1980.
- [27] Viacheslav Leonidovich Girko. *Theory of stochastic canonical equations*, volume 535. Springer Science & Business Media, 2001.
- [28] Oded Goldreich. *Introduction to property testing*. Cambridge University Press, 2017.
- [29] Friedrich Götze, Alexander Tikhomirov, et al. Rate of convergence in probability to the marchenko-pastur law. *Bernoulli*, 10(3):503–548, 2004.
- [30] Christoph Hafemeister and Rahul Satija. Normalization and variance stabilization of single-cell rna-seq data using regularized negative binomial regression. *Genome biology*, 20(1):1–15, 2019.
- [31] Donna K Harman. *The first text retrieval conference (TREC-1)*, volume 500. US Department of Commerce, National Institute of Standards and Technology, 1993.
- [32] Peter D Hoff. Model averaging and dimension selection for the singular value decomposition. *Journal of the American Statistical Association*, 102(478):674–685, 2007.
- [33] David Hong, Laura Balzano, and Jeffrey A Fessler. Asymptotic performance of pca for high-dimensional heteroscedastic data. *Journal of multivariate analysis*, 167:435–452, 2018.
- [34] David Hong, Jeffrey A Fessler, and Laura Balzano. Optimally weighted pca for high-dimensional heteroscedastic data. *arXiv preprint arXiv:1810.12862*, 2018.
- [35] David Hong, Kyle Gilman, Laura Balzano, and Jeffrey A Fessler. Heppcat: Probabilistic pca for data with heteroscedastic noise. *arXiv preprint arXiv:2101.03468*, 2021.
- [36] David Hong, Yue Sheng, and Edgar Dobriban. Selecting the number of components in pca via random signflips. *arXiv preprint arXiv:2012.02985*, 2020.
- [37] Roger A Horn, Roger A Horn, and Charles R Johnson. *Topics in matrix analysis*. Cambridge university press, 1994.
- [38] Sinisa Hrvatin, Daniel R Hochbaum, M Aurel Nagy, Marcelo Cicconet, Keiramarie Robertson, Lucas Cheadle, Rapolas Zilionis, Alex Ratner, Rebeca Borges-Monroy, Allon M Klein, et al. Single-cell analysis of experience-dependent transcriptomic states in the mouse visual cortex. *Nature neuroscience*, 21(1):120–129, 2018.
- [39] Martin Idel. A review of matrix scaling and sinkhorn’s normal form for matrices and positive maps. *arXiv preprint arXiv:1609.06349*, 2016.
- [40] J Edward Jackson. *A user’s guide to principal components*, volume 587. John Wiley & Sons, 2005.
- [41] Timothy M Johanson, Hannah D Coughlan, Aaron TL Lun, Naiara G Bediaga, Gaetano Naselli, Alexandra L Garnham, Leonard C Harrison, Gordon K Smyth, and Rhys S Allan. Genome-wide analysis reveals no evidence of trans chromosomal regulation of mammalian immune development. *PLoS genetics*, 14(6):e1007431, 2018.

- [42] Norman L Johnson, Adrienne W Kemp, and Samuel Kotz. *Univariate discrete distributions*, volume 444. John Wiley & Sons, 2005.
- [43] Iain M Johnstone and Debashis Paul. Pca in high dimensions: An orientation. *Proceedings of the IEEE*, 106(8):1277–1292, 2018.
- [44] IM Johnstone and Boaz Nadler. Roy’s largest root test under rank-one alternatives. *Biometrika*, 104(1):181–193, 2017.
- [45] Zheng Tracy Ke, Yucong Ma, and Xihong Lin. Estimation of the number of spiked eigenvalues in a covariance matrix by bulk eigenvalue matching analysis. *arXiv preprint arXiv:2006.00436*, 2020.
- [46] Philip A Knight. The sinkhorn–knopp algorithm: convergence and applications. *SIAM Journal on Matrix Analysis and Applications*, 30(1):261–275, 2008.
- [47] Shira Kritchman and Boaz Nadler. Determining the number of components in a factor model from limited noisy data. *Chemometrics and Intelligent Laboratory Systems*, 94(1):19–32, 2008.
- [48] Boris Landa. Scaling positive random matrices: concentration and asymptotic convergence. *arXiv preprint arXiv:2012.06393*, 2020.
- [49] Ken Lang. Newsweeder: Learning to filter netnews. In *Proceedings of the Twelfth International Conference on Machine Learning*, pages 331–339, 1995.
- [50] Rafał Łatała. Some estimates of norms of random matrices. *Proceedings of the American Mathematical Society*, 133(5):1273–1282, 2005.
- [51] William Leeb. Matrix denoising for weighted loss functions and heterogeneous signals. *arXiv preprint arXiv:1902.09474*, 2019.
- [52] William Leeb. Rapid evaluation of the spectral signal detection threshold and stieltjes transform. *arXiv preprint arXiv:1904.11665*, 2019.
- [53] William Leeb and Elad Romanov. Optimal spectral shrinkage and pca with heteroscedastic noise. *arXiv preprint arXiv:1811.02201*, 2018.
- [54] Lydia T Liu, Edgar Dobriban, Amit Singer, et al. e pca: high dimensional exponential family pca. *Annals of Applied Statistics*, 12(4):2121–2150, 2018.
- [55] Vladimir A Marčenko and Leonid Andreevich Pastur. Distribution of eigenvalues for some sets of random matrices. *Mathematics of the USSR-Sbornik*, 1(4):457, 1967.
- [56] Andrew D McRae and Mark A Davenport. Low-rank matrix completion and denoising under poisson noise. *arXiv preprint arXiv:1907.05325*, 2019.
- [57] Carl N Morris. Natural exponential families with quadratic variance functions. *The Annals of Statistics*, pages 65–80, 1982.
- [58] Carl N Morris. Natural exponential families with quadratic variance functions: statistical theory. *The Annals of Statistics*, pages 515–529, 1983.
- [59] Boaz Nadler et al. Finite sample approximation results for principal component analysis: A matrix perturbation approach. *The Annals of Statistics*, 36(6):2791–2817, 2008.
- [60] Art B Owen, Patrick O Perry, et al. Bi-cross-validation of the svd and the nonnegative matrix factorization. *The annals of applied statistics*, 3(2):564–594, 2009.
- [61] Debashis Paul. Asymptotics of sample eigenstructure for a large dimensional spiked covariance model. *Statistica Sinica*, pages 1617–1642, 2007.
- [62] Friedrich Pukelsheim. Biproportional scaling of matrices and the iterative proportional fitting procedure. *Annals of Operations Research*, 215(1):269–283, 2014.
- [63] Geneviève Robin, Julie Josse, Éric Moulines, and Sylvain Sardy. Low-rank model with covariates for count data with missing values. *Journal of Multivariate Analysis*, 173:416–434, 2019.
- [64] Joseph Salmon, Zachary Harmany, Charles-Alban Deledalle, and Rebecca Willett. Poisson noise reduction with non-local pca. *Journal of mathematical imaging and vision*, 48(2):279–294, 2014.
- [65] Abhishek Sarkar and Matthew Stephens. Separating measurement and expression models clarifies confusion in single-cell rna sequencing analysis. *Nature Genetics*, 53(6):770–777, 2021.

- [66] Haipeng Shen and Jianhua Z Huang. Analysis of call centre arrival data using singular value decomposition. *Applied Stochastic Models in Business and Industry*, 21(3):251–263, 2005.
- [67] Richard Sinkhorn. Diagonal equivalence to matrices with prescribed row and column sums. *The American Mathematical Monthly*, 74(4):402–405, 1967.
- [68] Richard Sinkhorn. Diagonal equivalence to matrices with prescribed row and column sums. ii. *Proceedings of the American Mathematical Society*, 45(2):195–198, 1974.
- [69] Richard Sinkhorn and Paul Knopp. Concerning nonnegative matrices and doubly stochastic matrices. *Pacific Journal of Mathematics*, 21(2):343–348, 1967.
- [70] Hanna M Wallach. Topic modeling: beyond bag-of-words. In *Proceedings of the 23rd international conference on Machine learning*, pages 977–984, 2006.
- [71] Svante Wold. Cross-validatory estimation of the number of components in factor and principal components models. *Technometrics*, 20(4):397–405, 1978.
- [72] Jianfeng Yao, Shurong Zheng, and ZD Bai. *Sample covariance matrices and high-dimensional data analysis*. Cambridge University Press Cambridge, 2015.
- [73] Yong-Qua Yin, Zhi-Dong Bai, and Pathak R Krishnaiah. On the limit of the largest eigenvalue of the large dimensional sample covariance matrix. *Probability theory and related fields*, 78(4):509–521, 1988.
- [74] Anru Zhang, T Tony Cai, and Yihong Wu. Heteroskedastic pca: Algorithm, optimality, and applications. *arXiv preprint arXiv:1810.08316*, 2018.
- [75] Grace XY Zheng, Jessica M Terry, Phillip Belgrader, Paul Ryvkin, Zachary W Bent, Ryan Wilson, Solongo B Ziraldo, Tobias D Wheeler, Geoff P McDermott, Junjie Zhu, et al. Massively parallel digital transcriptional profiling of single cells. *Nature communications*, 8(1):1–12, 2017.